

Quantification of coastal bank erosion rates in Western Port

Kerrie Tomkins¹, Gordon McLachlan¹ and Rhys Coleman²

¹CSIRO Land and Water; ²Melbourne Water

Final report

April 2014

Australia is founding its future on science and innovation. Its national science agency, CSIRO, is a powerhouse of ideas, technologies and skills.

CSIRO initiated the National Research Flagships to address Australia's major research challenges and opportunities. They apply large scale, long term, multidisciplinary science and aim for widespread adoption of solutions. The Flagship Collaboration Fund supports the best and brightest researchers to address these complex challenges through partnerships between CSIRO, universities, research agencies and industry.

The Water for a Healthy Country Flagship aims to provide Australia with solutions for water resource management, creating economic gains of \$3 billion per annum by 2030, while protecting or restoring our major water ecosystems. The work contained in this report is collaboration between CSIRO and Melbourne Water.

For more information about Water for a Healthy Country Flagship or the National Research Flagship Initiative visit www.csiro.au/org/HealthyCountry.html

Citation

Tomkins K, McLachlan G and Coleman R (2014) Quantification of coastal bank erosion rates in Western Port. CSIRO Water for a Healthy Country Flagship, Australia.

Copyright and disclaimer

© 2014 Melbourne Water Corporation. To the extent permitted by law, all rights are reserved and no part of this publication covered by copyright may be reproduced or copied in any form or by any means except with the written permission of Melbourne Water Corporation.

Important disclaimer

CSIRO advises that the information contained in this publication comprises general statements based on scientific research. The reader is advised and needs to be aware that such information may be incomplete or unable to be used in any specific situation. No reliance or actions must therefore be made on that information without seeking prior expert professional, scientific and technical advice. To the extent permitted by law, CSIRO (including its employees and consultants) excludes all liability to any person for any consequences, including but not limited to all losses, damages, costs, expenses and any other compensation, arising directly or indirectly from using this publication (in part or in whole) and any information or material contained in it.

Contents

Acknowledgments.....	v
Executive summary	vi
1 Introduction	1
1.1 Background and aims.....	1
1.2 Physiography of the bay	3
1.3 Lang Lang coastline.....	4
1.4 Historical changes at Lang Lang	5
2 Methods.....	8
2.1 DGPS and GPS field surveys of the Lang Lang coastline	8
2.2 Aerial photograph interpretation.....	9
2.3 Selection of an erosion monitoring site.....	10
2.4 Installation of erosion pins and tape and clinometer surveys.....	11
2.5 Installation of a monitoring camera and weather station.....	12
2.6 Installation of a groundwater piezometer and tide gauge.....	15
2.7 Sediment sampling and laboratory analysis	15
2.8 Fetch and wave modelling.....	17
3 Results.....	19
3.1 Morphology and sedimentology of the banks.....	19
3.2 Long-term estimates of bank erosion rates using aerial photographs, GPS surveys and LIDAR.....	24
3.3 Bank erosion rates during the monitoring period: November 2012 to November 2013	29
3.4 Characteristics of storms and tides during the monitoring period	37
3.5 Analysis of wind conditions, fetch and wave energy.....	39
3.6 Examination of trends in groundwater levels in the banks	50
4 Summary and management implications	52
4.1 Summary of new knowledge of sediment inputs from bank erosion	52
4.2 Further work	54
4.3 Options and recommendations for reducing erosion at Lang Lang	54
4.4 Implications for other eroding areas around Western Port.....	58
References.....	60

Figures

Figure 1. Western Port showing the major areas of coastal erosion in red identified from the latest Google Earth imagery. Coastal erosion includes beach erosion, erosion of sand dunes on the foreshore and erosion of clay banks such as at the monitoring site near Lang Lang.	1
Figure 2. 1888 Department of Crown Lands and Survey Yallock Parish map, showing the Lang Lang River channel (bottom-right), Yallock Creek (top-centre) and a strongly crenulated coastline. The approximate location of the monitoring site is indicated by the red arrow.....	7
Figure 3. Typical bank profile where the vegetation and uppermost sediment has been stripped back from the bank edge exposing a distinctive thin reddish unit overlying massive grey clays. The true edge of the banks is indicated by the red arrow.	9
Figure 4. View of the monitoring site at low tide looking north. In the image is a small crenulation with steeply sloping upper banks, a lower bench of ~ 0.5 m high, eroded material on the tidal flats (clay balls) and vertical-benched banks in the distance.....	11
Figure 5. Example of one of the erosion pin transects, showing the geomorphic units identified. The units were also used to classify the heights reached during each high tide.....	12
Figure 6. Monitoring camera, solar panels and weather station installed at the site.	13
Figure 7. Examples of the classification system used to characterise the wave conditions during each high tide.	14
Figure 8. Left: Bank profile sampled at the monitoring site showing 4 of the 5 sedimentary layers and prominent surface cracking. Right: Bank profile near the Lang Lang River, with a large piece of buried wood marking the boundary between a red-brown organic-rich clay layer and the lowermost grey clay unit.	17
Figure 9. Generic classification of bank slope profiles (Source: Crouch, 1987).	19
Figure 10. Classification of bank profiles between the Yallock Drain and the Lang Lang River.....	20
Figure 11. Snap-shot of the historical air photo analysis showing the smoothing of the headlands and retreat of the banks over time. Labels are as follows: 'A' indicates the general area where there has been pronounced smoothing of headlands and crenulations over time; 'B' indicates areas of enhanced erosion due to the drain outlets; 'C' indicates the very large crenulations which are, or have in the past, threatened the sea wall. The air photo mapping indicates the position of the upper edge of the banks.	26
Figure 12. Change in the position of the upper edge of the banks at the monitoring site between 1947, 1977, 1984, 2008, 2012 and 2013. The location of the first pin in each erosion pin profile is also shown.....	27
Figure 13. Erosion monitoring site showing the edge of the banks (jagged black line) and edge of the lower bench (light blue line) as surveyed in October 2012. The location of the first erosion pin in each profile, camera, groundwater piezometer, tide gauge and bank profile analysed are also shown. The image in the background is a 2008-9 air photo which shows some sand deposition on the bench surface and floodplain at the centre of the crenulation. The air photo also shows the position of the edge of the bench and top of the banks in 2008-9. The length of the coastline from BankProfile to Tag18 is 175 m.....	30
Figure 14. Total average sediment loss per erosion pin profile since the start of monitoring.....	31
Figure 15. Trends in sediment loss across 8 of the 12 profiles showing parallel retreat of the steeper sub-vertical parts of the banks and minimal downwards erosion of the floodplain and bench surface. Profiles 50, 60, 70 and 90 (not shown) are similar to profiles 50 and 80. The surveys	

of profiles 18 and 00 show some variability in chronology, particularly on the bench, due to the dislodgement of some pins and re-setting of the transects in as close to their original position as possible. Note the long wave run-up on the bench surface in Profiles 30 to 80.	35
Figure 16. Patterns of average daily wind speed and direction at the monitoring site (~ 13 months data), Cerberus (22 years data) and Rhyll (22 years data). The stacked colours represent increasing wind speeds, while the length of the bars indicates the proportion of winds from each direction.....	39
Figure 17. Patterns of highest daily wind speeds at the monitoring site (~ 13 months data), Cerberus (22 years data) and Rhyll (22 years data). The stacked colours represent increasing wind speeds, while the length of the bars indicates the proportion of winds from each direction.	40
Figure 18. Seasonal trends in daily wind speed and direction at the monitoring site, Cerberus and Rhyll. The stacked colours represent increasing wind speeds, while the length of the bars indicates the proportion of winds from each direction.	41
Figure 19. Differences in wind speed and direction at the monitoring site between erosion pin measurements. The stacked colours represent increasing wind speeds, while the length of the bars indicates the proportion of winds from each direction.	42
Figure 20. Patterns of fetch for each wind direction. The scale for all plots is shown in the plot labelled 000, while M is Monitoring site, JJ is Jam Jerrup and G is Grantville. The areas of the bay that have the longest fetch are indicated by red-orange, while dark blue indicates the shortest fetch. Note how these patterns change with wind direction.	43
Figure 21. Summary of the seasonal wind patterns and fetch for each direction at the monitoring site. The data shows that winds from the W and WSW in autumn and spring have the longest fetch, followed by winds from the WNW in winter (& spring and autumn) and southerly winds in summer (& spring and autumn). Winds from these directions have the potential to generate greater wave heights compared to winds of similar speeds from different directions. The light winds from the ~ NE that were recorded throughout the year, have ~ zero fetch and hence no impact on erosion at the monitoring site.	45
Figure 22. Maximum wave power predictions for different wind speeds (10–100 km h ⁻¹) and directions at the monitoring site, Jam Jerrup and Grantville, assuming a water depth of 2 m which is equivalent to the maximum high tide recorded. The wave power predictions for winds from the NE, ENE, E, ESE and SE are not shown since these values are < 0.1 kW m ⁻¹ for all wind speeds.....	46
Figure 23. Total daily wave power at the monitoring site, Jam Jerrup and Grantville. Wave power was calculated using the wind speed-direction and tide data, and modelled fetch and wave heights. Data gaps shown in the plots are due to gaps in the wind speed-direction data. These were due to occasional problems with the weather station.	47
Figure 24. Sediment loss versus wave power at the monitoring site, summed to represent totals for the erosion pin measurement periods. The data show a weak positive relationship between sediment loss and wave power.	48
Figure 25. Sediment loss and total wave power for each erosion pin measurement period at the monitoring site, compared to monthly trends in evaporation recorded at the nearby CSIRO Aspendale station.....	49
Figure 26. Sediment loss versus evaporation recorded at the nearby CSIRO Aspendale station. The orange line indicates the trend through all the data. The black line indicates the trend through the data coloured black, excluding the two orange points which represent the 23 April and 14 October erosion pin measurements. With the exception of the April and October measurements, there is a very good correlation between sediment loss and evaporation, with evaporation affecting the degree of cracking of the surface through shrink-swell of the clays. For the April and October	

measurements, in addition to evaporation, other factors such as wave power appear to influence erosion rate.50

Figure 27. Groundwater levels, tide heights and rainfall at the monitoring site. Note, the groundwater data were corrected for AHD so that they are directly comparable with the tide data.....51

Tables

Table 1. Relevant research papers on Western Port published in the 1970s – 80s.....2

Table 2. Chronology of sea level changes and geomorphic response in Western Port in the late Quaternary (Source: Marsden and Mallett, 1975).....4

Table 3. Chronology of significant changes to the Lang Lang coastline and Tobin Yallock Swamp.....6

Table 4. Air photos used to calculate long-term erosion rates and examine long-term changes in the shape of the shoreline.9

Table 5. Sedimentology of the bank material.22

Table 6. Long-term rates of sediment loss and sediment yield between the Yallock Drain and Lang Lang River.28

Table 7. Average rates of sediment loss measured from the erosion pins over the 12 months (392 days) of monitoring.31

Table 8. Variability in erosion by geomorphic unit. Erosion is indicated by negative values, while deposition is indicated by positive values.....32

Table 9. Maximum wave position reached during high tides, expressed as a percentage of the total events recorded by the monitoring camera between 1 November 2012 and 25 November 2013.....37

Table 10. Maximum wave size during high tides, expressed as a percentage of the total events recorded by the monitoring camera. Examples of the wave categorisation used are shown in Fig. 7.....38

Table 11. Maximum wave position reached during high tides under calm conditions, expressed as a percentage of the total number of events under calm conditions.38

Table 12. Management options to reduce erosion of the banks at Lang Lang and reduce sediment inputs into Western Port.....56

Acknowledgments

This study was commissioned by Melbourne Water who provided funding for the research. We thank Jen Austin for assistance with the DEMs, Arthur Reed for running the Fetch-Wave model and extracting the site-based results, and Gary Hancock and Tom Hurst for coming out to the field site on occasions to assist with field work. We also gratefully acknowledge Scott Wilkinson and Phillip Ford for their helpful reviews of the draft report, as well as valuable on-going discussion and feedback throughout the project.

Executive summary

This report presents the findings from a 12-month monitoring project that investigated the rates, processes and spatial distribution of coastal bank erosion in Western Port, Victoria (also referred to as Westernport Bay, the bay). The project was commissioned by Melbourne Water in 2012 to address a high priority research need relating to the contribution of coastal erosion to sediment inputs in the bay. The focus of the study is an 8.6 km stretch of coastline west of Lang Lang that had been identified as an erosion hot-spot in the bay. Previous work at the site included a sediment tracer study by the CSIRO (Wallbrink *et al.* 2003), which had estimated that the banks were supplying up to 32 % of the fine sediment in the bay, compared to 68 % from catchment sources.

This study aimed to address several key research questions on the rates, processes and conditions facilitating bank erosion by measuring and quantifying the amount of sediment eroded over 12 months at a monitoring site, set in context with historical records and observations. The monitoring site is a small bay and headlands, reflecting the typical morphology of the Lang Lang coastline. Monitoring equipment comprising 100 erosion pins organised into 12 profiles, a live-stream camera, weather station, piezometer and tide gauge were installed at the site in late 2012. The erosion pins were measured at approximately monthly intervals to provide data on sediment loss over time, while the camera images, weather station and gauges recorded the prevailing wind/storm/tide conditions at 30-minute intervals. The erosion pin measurements were combined with tape and clinometer surveys of the banks during each field visit to examine changes in the shape of the banks over time. DGPS and GPS surveys of the 8.6 km coastline were also carried out at the start and end of the project to determine the amount of erosion over 12 months, in comparison to an analysis of historical air photos dating back to 1947. A sedimentological analysis of the bank material was undertaken to determine sediment characteristics and erosional susceptibility of the banks. Simple fetch and wave modelling were also undertaken to investigate the importance of wave power on erosion rates.

The results showed that the shape of the banks is strongly controlled by sediment characteristics. Five different soil layers were identified, which form 5 different geomorphic units (floodplain, bank crest, upper-lower banks, bench surface and bench face). However, all layers have a relatively high clay content (av. 59 %), low dispersibility, and low-moderate erosional susceptibility. Erosion of the banks is occurring by parallel retreat of the steeper sub-vertical parts through the physical processes of abrasion and quarrying (plucking) of sediment as a result of wave action. Erosion is enhanced by bioturbation holes and tunnels in the sediments, and wetting and drying of the surface over the tidal cycle. The net result is the release of significant quantities of fine sediment (clay and silt) into the bay (~80 %) as well as fine sand (~20 %) and organic matter (~< 10 %).

Average erosion rates measured over the 12 months of monitoring were 2.6 cm mth⁻¹ or 0.31 m yr⁻¹. This is consistent with the long-term average erosion rate determined from aerial photographs of 0.42 m yr⁻¹ over 65 years. Higher rates of erosion were recorded on the headlands in comparison to the crenulation at the monitoring site, which is consistent with long-term trends from the aerial photos that show an overall smoothing of the coastline since at least 1947. We estimate that from 8.6 km of coastline, the area of sediment loss to the bay over 65 years is 233,000 m², which equates to an average sediment yield of 4.2 ± 2.9 kt yr⁻¹ and an overall sediment input of 270 kt since 1947. However, there is significant spatial and temporal variability in erosion. In some years, maximum bank erosion rates could potentially equal or exceed 1 m yr⁻¹ and sediment yields could be more than double the average.

The major controls on erosion rates at Lang Lang and around Western Port are: i) sediment characteristics, ii) orientation of the coastline relative to the dominant wind-wave directions and the direction of longest fetch, iii) high frequency inundation through the tidal cycle, iv) seasonal wind patterns with winds predominantly from a westwards direction (i.e. NNW, NW.. to S), and v) seasonal evaporation affecting the degree of wetting-drying and cracking of the bank surface. Controls ii) to iv) determine wave energy and the magnitude of wave power on the bank surface, while sediment characteristics and seasonal evaporation determine the resistance of the banks to erosion.

Erosion is occurring along the 8.6 km of banks at Lang Lang due to a combination of continuous erodible sedimentary units and exposure of the shoreline to strong wind-generated waves facilitated by the seasonal westerly wind patterns and a long fetch. During the majority of high tides, the banks are being subject to wave attack which results in small but continuous daily erosion and, over time amounts to substantial erosion and sediment inputs into the bay. This study has highlighted some areas for further work, including examination of the importance of seasonal evaporation on the degree of cracking of the bank surface through wetting-drying, establishment of wave power thresholds and investigation of the importance of wave direction on erosion rates. There was no evidence from the monitoring sites that storm events caused significantly greater erosion, however determining these thresholds and wave impacts is an important precursor for the design of effective erosion control structures.

To reduce erosion of the banks at Lang Lang and at other areas around the bay, a number of management options may be considered, that address the physical erosion processes on the banks and/or reduce wave energy in the near shore area. These options include revegetation and installation of engineering structures on or off-shore of the banks, taking into consideration areas of highest erosion (e.g. headlands, sections with high sinuosity) or where the sea wall is most vulnerable. Quantitative assessment of the options was beyond the scope of this study but should be undertaken. Additional work could also consider the likelihood of potential changes in erosion rates due to climate change impacts on wind-wave patterns and sea level.

1 Introduction

1.1 Background and aims

In a recent review of environmental knowledge to guide the strategic management of Western Port, several high priority research gaps were identified (Melbourne Water, 2011). One of the priorities was to estimate the contribution of coastal erosion to nutrient and sediment budgets in the bay (Fig. 1). This priority was in the context of poor water quality, specifically high turbidity levels around the head of the embayment, and observed loss of seagrass beds over recent decades. Integral to addressing the turbidity problem is having a good understanding of the sources of sediment in the bay. This information, along with knowledge of the rates and processes of coastal erosion, is also needed to determine appropriate management options for reducing sediment inputs.

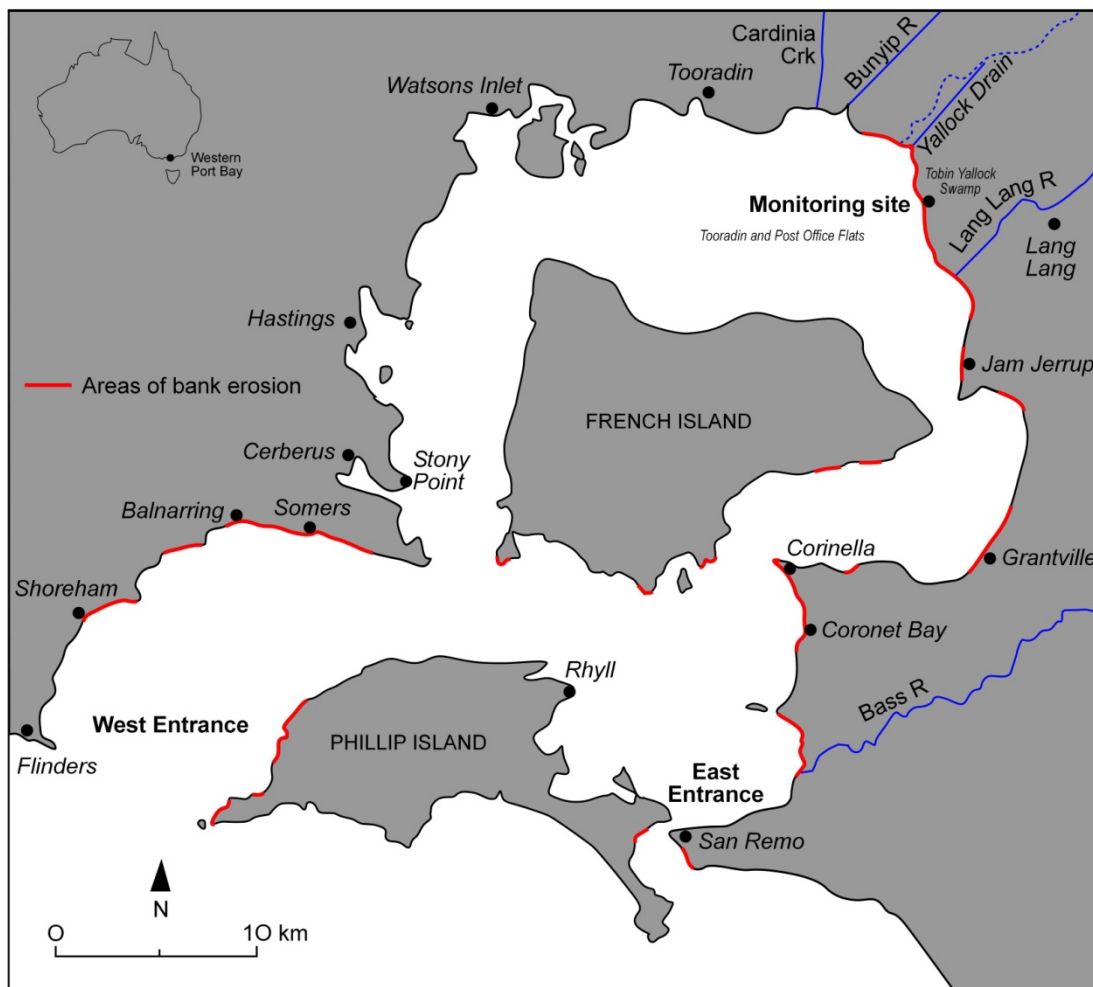


Figure 1. Western Port (also known as Westernport Bay) showing the major areas of coastal erosion in red identified from the latest Google Earth imagery. Coastal erosion includes beach erosion, erosion of sand dunes on the foreshore and erosion of clay banks such as at the monitoring site near Lang Lang.

To date, there has been limited research on coastal bank erosion in Western Port. A large body of work was done in the 1970s associated with the Western Port Environmental Study which is written up in a large volume (Shapiro, 1975) and published in several journal articles (see Table 1 for some relevant examples). These studies provided a baseline understanding of the biological and physical processes in the bay, in particular the distribution of mangroves and, water and sediment circulation patterns. Other work also investigated the interactions between sediment and seagrass. Two studies that focused on erosion of a section of the shoreline between Yallock Creek and the Lang Lang beach, provided good insights into how and why bank erosion is occurring (Gell, 1974) as well as an estimate of the average sediment yield over 90 years: 1.3 – 2.8 kt yr⁻¹ (Sargeant, 1977).

Table 1. Relevant research papers on Western Port published in the 1970s – 80s

THEME	AUTHORS
Mangroves and salt marsh	Bird (1971); Bird (1986)
Seagrass decline	Bulthuis (1983); Bulthuis <i>et al.</i> (1984)
Coastal processes and erosion	Gell (1974) (hons thesis); Marsden and Mallett (1975); Sargeant (1977); Marsden <i>et al.</i> (1979)
Geology	Thompson (1974); Spencer-Jones <i>et al.</i> (1975)
Historical changes	Bird and Barson (1975); Bird (1980)
Hydrogeochemistry of the bay and hydrodynamic modelling	Harris and Robinson (1979); Harris <i>et al.</i> (1979); Hinwood (1979); Hinwood and Jones (1979); Sternberg and Marsden (1979)
Western Port Bay Environmental Study	Butcher (1979); Shapiro and Connell (1975)

A series of studies were undertaken by the CSIRO in 2000-2003 focusing on sediment accumulation, sediment redistribution and sources of sediment in the bay (see Wallbrink *et al.*, 2003 and the technical reports therein). The CSIRO studies used geochemical sediment tracer techniques to estimate that the most significant source of fine sediment over recent decades was erosion of the clay banks at Lang Lang, accounting for up to 32 % of sediment inputs into the bay, or ~20 kt yr⁻¹. The remaining sediment was supplied by three main tributaries: Bunyip River (27 %), Cardinia Creek (21 %) and Lang Lang River (18 %), predominantly through channel bank and gully erosion. A more recent study by Hurst (2012) using historical aerial photographs commencing from 1973, estimated that the rates of bank retreat at Lang Lang were on average 0.5 m yr⁻¹ equating to an average sediment yield of 15.2 kt yr⁻¹ over 36 years. Hurst showed that the rates varied on decadal timescales, and some parts of the coastline such as the bays were eroding faster relative to the headlands and straight sections of banks.

This project aimed to build on previous work and address the need for quantitative information on the contribution of coastal erosion to nutrient and sediment budgets in Western Port. The project focuses on an 8.6 km section of coastline at Lang Lang as the primary study area, but other areas of erosion around the bay are also considered. The project commenced in July 2012, with erosion monitoring equipment installed at one site between the end of October and mid-December 2012. Data and observations were collected over a 12-month period to answer several key research questions, including:

1. What is the morphology, sedimentology and erosional susceptibility of the banks?
2. What are the rates of bank erosion over the study period and is there spatial and temporal variability in rates?
3. How do erosion rates determined in this study compare with previous estimates and longer term estimates derived from aerial photos?

4. What is the role of storm events and tides in triggering erosion, and reworking or removing eroded material?
5. How do the changes in pore water pressure associated with the semi-diurnal tidal cycle and groundwater seepage impact on the likelihood of bank failure?
6. Are other factors such as wave energy and orientation of the shoreline relative to the wind-wave direction important?
7. What are the options, if any, for reducing erosion rates?
8. What are the implications for other areas of bank erosion around Western Port?

This report addresses these questions by presenting the results from monitoring between 1 November 2012 and 25 November 2013. The monitoring involved installation of 100 x 1m erosion pins, a live-stream camera, Davis weather station, tide logger and a ground water piezometer. The study also utilised historical aerial photographs, GPS surveys, GIS analysis, sedimentological analysis and, fetch and wave modelling.

1.2 Physiography of the bay

Western Port is a bedrock-controlled coastal embayment (Westernport Bay) located ~70 km south-east of Melbourne. A number of small streams deliver fresh water and sediment inputs into the bay (Marsden and Mallett, 1975). The bay is characterised by two main arms: north and east, which are separated by French Island in the centre and the tidal divide in the north-east corner of the bay.

The bay is strongly tidal (semi-diurnal) with a normal range of 1.2 m, extending up to 3.3 m during spring tides (Marsden and Mallett, 1975). However, there are large differences in tide heights on a sub-daily and daily timescale, as well as a strong spring-neap difference (Sternberg and Marsden, 1979). Water circulation and sediment transport around the bay is strongly influenced by tidal processes. The net movement of water and suspended sediment is in a clockwise direction from the north arm to the east arm due to a phase lag between the north and east arm tides (Hinwood and Jones, 1979). Winds are also important in increasing wave heights, enhancing re-suspension of fine sediment from the intertidal zone and inducing bottom sediment transport (Sternberg and Marsden, 1979).

One of the most significant influences on the morphology, processes and long-term evolution of the bay is changes in sea level associated with marine transgressions and regressions during the late Quaternary (Marsden and Mallett, 1975) (see Table 2). In the last 20 ka, the shoreline of Western Port has changed markedly from being located outside of the bay at the Last Glacial Maximum, to being higher and possibly extending further inland in some areas at the height of the Last Interglacial ~6 ka. The bay environment has oscillated between marine and terrestrial, while the location of sediment deposition and erosion has also changed over time. The present shoreline has been in place for less than ~2 ka and is currently characterised by erosional and depositional features including: cliffs, banks and bluffs; sandy shorelines and beaches; and intertidal flats comprising salt marsh, mangroves and mud flats (Bird and Barson, 1975; Marsden et al., 1979). Where erosion is occurring, it is reworking older marine, terrestrial (swamp, floodplain) and aeolian (sand dune) sediments, and bedrock, which form the present margin of the bay.

Table 2. Chronology of sea level changes and geomorphic response in Western Port in the late Quaternary (Source: Marsden and Mallett, 1975)

TIME (BEFORE PRESENT)	SEA LEVEL	BAY ENVIRONMENT	GEOMORPHIC RESPONSE
125 ka (Penultimate Interglacial)	High, probably similar or slightly lower than present	Marine	Extensive fluvial deposition of Heath Hill Silt and Cardinia Sand.
18-20 ka (Last Glacial Maximum)	Low, possibly 27 m lower than present.	Terrestrial	Erosion and channel entrenchment into older sediments. Aeolian deposition of Cranbourne sands.
6-10 ka	Rising	Terrestrial to marine	Drowning of the bay including aeolian sands. Marine reworking of sediments.
5-6 ka (Last Interglacial)	High, 1-2 m above present	Marine	Progradation of sand barriers and beaches. Extensive swamp development and drainage disruption on adjacent plains including Koo Wee Rup swamp.
5 ka – 1800s	Falling	Marine	Abandonment of near shore features. Progradation of salt marshes, mangroves and tidal flats.
1800s – present	Rising due to climate change	Marine	Extensive fluvial and coastal modification including swamp drainage and channelisation.

1.3 Lang Lang coastline

The embayment head, located in the north-east corner of Western Port, is characterised by prominent, eroding 1 - 2 m high alluvial banks that extend between Yallock Creek and the northern end of Lang Lang beach, a distance of 11.5 km. The coastline is crenulated in plan-view, being characterised by narrow headlands and small bays. The erosion and crenulated patterns were first noted in the early surveyors charts of 1827 (Captain Wetherall), 1842 (George Smythe) and 1865 (Henry Cox). Smythe (1842) described the embayment head as an erosional shoreline with numerous rills of freshwater draining the adjacent tea-tree swamp but no defined channel outlets draining into the bay. The area was also noted for its lack of mangroves in comparison to the rest of the bay.

North of Yallock Creek is a section known as The Inlets, which includes the Bunyip River outlet and is characterised by a wide strip of mangroves and salt marsh marking the landward side of the intertidal zone. South of Lang Lang beach is Red Bluff and Stockyard Point which are characterised by beach sands, high cliffs and a series of prograding beach ridges and bars.

On the bay-ward side of the Lang Lang shoreline are the Tooradin and Post Office tidal flats which feature small dendritic channel patterns extending across the tidal divide and shallow, low energy ebb-flow channels which drain into the north and east arms (Sternberg and Marsden, 1979). Sediments in the embayment head are characterised by clay, silt and very-fine to medium sands sourced locally from erosion of the clay banks and from tributary inputs, as well as landward transport of fine suspended sediment within the bay (Marsden and Mallett, 1975; Sternberg and Marsden, 1979; Wallbrink et al., 2003). Following catchment disturbance, increasing sediment loads in the Bunyip River and Lang Lang River led to the progradation of fan-like sand sheets over the tidal flat sediments at the river outlets (Bird and Barson, 1975). During low tide, these tidal flats are exposed and the sediments are subjected to bioturbation by mud-dwelling organisms such as crabs and polychaetes (marine worms) (Marsden and Mallett, 1975).

On the land-ward side of the Lang Lang shoreline is the former Tobin Yallock Swamp, which was originally colonised by dense swamp vegetation comprising *Melaleuca ericafolia* (Swamp Paperbark), *Juncus spp.* and *Phragmites australis* (Common Reed) prior to clearing in the mid 1800s (Gell, 1974). The swamp area is relatively flat lying and extensive, comprising an area of ~15 km². The sedimentology is generally referred to as peats and peaty clays but is poorly described (e.g. Gell, 1974). Prior to human disturbance, the Lang Lang River discharged into a small open lake at the apex of the swamp, with swamp waters overflowing the banks probably through rills similar to those described in the early surveyors charts (Gell, 1974).

1.4 Historical changes at Lang Lang

There is a well documented history of post-european (1798+) landuse change and drainage modification in the Lang Lang area based on old surveys, aerial photographs and anecdotal evidence (e.g. Gell, 1974; Bird and Barson, 1975; Bird, 1980) (see Table 3). Of particular interest are the early surveyors charts and the first parish map (Victoria Department of Crown Lands and Survey, 1888) which shows a strongly crenulated coastline and a small very sinuous channel to the north identified as Yallock Creek (Fig. 2). These historical maps are of major significance because they provide clear evidence that erosion of the coastline pre-dates european disturbance in the catchment and adjacent swamp land. The maps also show also that there has been very little change to the general outline of the shoreline since at least the mid 1800s. This implies that the bank erosion is a natural process in the bay, although it may be exacerbated by vegetation clearing, swamp drainage and seagrass decline. The maps show that there was thick tea tree swamp extending to the top of the banks and mangroves were notably absent on the tidal flats near Lang Lang, including across the drainage divide in the bay (Table 3). However, it is unclear whether the tidal flats and deeper areas were colonised by seagrass, which may affect wave propagation, during this time.

The first person to make significant changes to the land around Lang Lang was William Lyall in the 1860s who attempted to drain the Tobin Yallock Swamp and cut a channel for the Lang Lang River to the coast (Bird, 1980). Other drainage channels were also cut including the 9ft Yallock drain and the 20 ft Monomeith drain which are still operational today (Gell, 1974). The cutting of drainage lines, straightening of channels and subsequent dredging from the early 1910s to increase channel capacity was designed to improve drainage efficiency, reduce flooding and reduce waterlogging in the reclaimed swamp land. But it also resulted in a number of adverse impacts. In particular, channel incision through knickpoint retreat was initiated in the Lang Lang River and Bunyip Creek (Bird, 1980). The knickpoints retreated tens of kilometers upstream releasing significant volumes of sediment into the bay over periods of decades (Bird, 1980).

Other significant changes since settlement include the construction of a sea wall in 1916 which runs approximately parallel for the length of the coastline from the Yallock Drain to Lang Lang beach (Bird, 1980). The wall was constructed to prevent incursion of sea water from the bay during high spring tides and storm events. Some parts of the wall have been subsequently modified, reinforced or realigned due to erosion, such as at the Lang Lang River outlet and south of the Monomeith Drain, but most of the original wall is still in place. The sea wall also forms an important chronological marker in investigating historical changes to the coastline over time.

Lyall was also the first to clear the swamp of vegetation inland of the coastline (Gell, 1974) and presumably vegetation removal up to the edge of the banks had occurred by the time of construction of the sea wall (i.e. within 50 years).

Table 3. Chronology of significant changes to the Lang Lang coastline and Tobin Yallock Swamp.

YEAR	CHRONOLOGY	SOURCE
1827	Map: Captain Wetherall, H.M.S. Fly. Chart of Western Port in Bass's Straits (scale 1:88,704) – shows thick tea tree swamp, drained by a small defined channel.	Wetherall, 1827 (map)
Late 1830s	First squatters arrive and graze the Tobin Yallock Swamp	Bird, 1980
1842	Map: George Smythe, Survey of the eastern coast of Western Port (scale 1:31,679) – describes numerous rills of freshwater draining the Tobin Yallock Swamp, but no channels draining into the bay.	Shown in Gell, 1974
1865	Map: Henry Cox, Western Port (scale 1:36,457) – shows navigational features including channels, shoals and the distribution of mangroves around the bay.	Described in Bird and Barson, 1975
1865-1870	Start of drainage works through Tobin Yallock Swamp: Construction of 3 major drains – 9 ft Yallock drain, 20 ft Monomeith Drain (Roads Board) and 12 ft Lang Lang Drain (Lyall). Construction of several minor drains through tea-tree scrub (Lyall).	Gell, 1974
1886	Cutting of a continuous channel for the Lang Lang River from Heath Hill to Western Port; start of channel incision.	Bird, 1980
1887	Map: William Lyall – shows dense tea-tree scrub to edge; land cleared and drained further inland.	Shown in Gell, 1974
1888	Map (Figure 2): Victorian Dept of Crown Lands and Survey, Yallock, County of Mornington (scale 1:31,680) – shows a significantly crenulated coast and the Lang Lang Drain. The Monomeith Drain and Yallock Drain are not shown.	Dept of Crown Lands and Survey, 1888 (map)
1910	Public Works Department starts desnagging the Lang Lang channel leading to further flooding.	Bird, 1980
1912	First sea wall around the Lang Lang shore constructed by Mr Nelson.	Bird, 1980
1914	Start of erosion in the Main Drain (Bunyip Creek) – erosion continues for ~ 20 years.	Gell, 1974
1916	Public Works Department build a more substantial sea wall to prevent flooding of adjacent agricultural land by sea water.	Bird, 1980
1912-1916	Excavators dredge the lower 3 kms of the Lang Lang channel from the South Gippsland Highway to the shoreline. Channel enlarged to 12 x 2.5 m – known as the Catani channel. Lyalls' channel becomes the outlet for Adams Creek.	Gell, 1974; Bird, 1980
1922-23	Two dredges used to deepen, straighten and embank the Lang Lang River at Yallock.	Bird, 1980
1920s – 1930s	Significant period of incision in the lower Lang Lang channel.	Bird, 1980
1925	Start of the Lang Lang R gauge.	Bird, 1980
1934	Major floods affect the Koo Wee Rup area.	Anecdotal evidence (Koo Wee Rup pub)
1937	Levee banks constructed along the Lang Lang R channel from the highway to the shoreline to prevent flooding of adjacent paddocks.	Gell, 1974
Post- 1937 evidence from air photos (see Table 4 for air photo details):		
Btw 1947 and 1973	Relocation of the sea wall at the Lang Lang R outlet and near the Yallock drain.	1947 & 1973 air photos

YEAR	CHRONOLOGY	SOURCE
1973	The sea wall is under threat from erosion in three places north and south of the monitoring site.	1973 air photo
1984	Several areas of the sea wall are under threat from erosion including the main drain outlets. The sea wall has been partly breached in 5 places.	1984 air photo
Btw 1990 and 2008	Relocation of the sea wall immediately north of the monitoring site	1990 air photo and 2008 DEM
2012/13	Many areas of the sea wall are under erosion threat. Landholders have put in place revetment works composed of building waste materials to prevent further erosion. Some of these revetment works are being undermined in places.	Field evidence

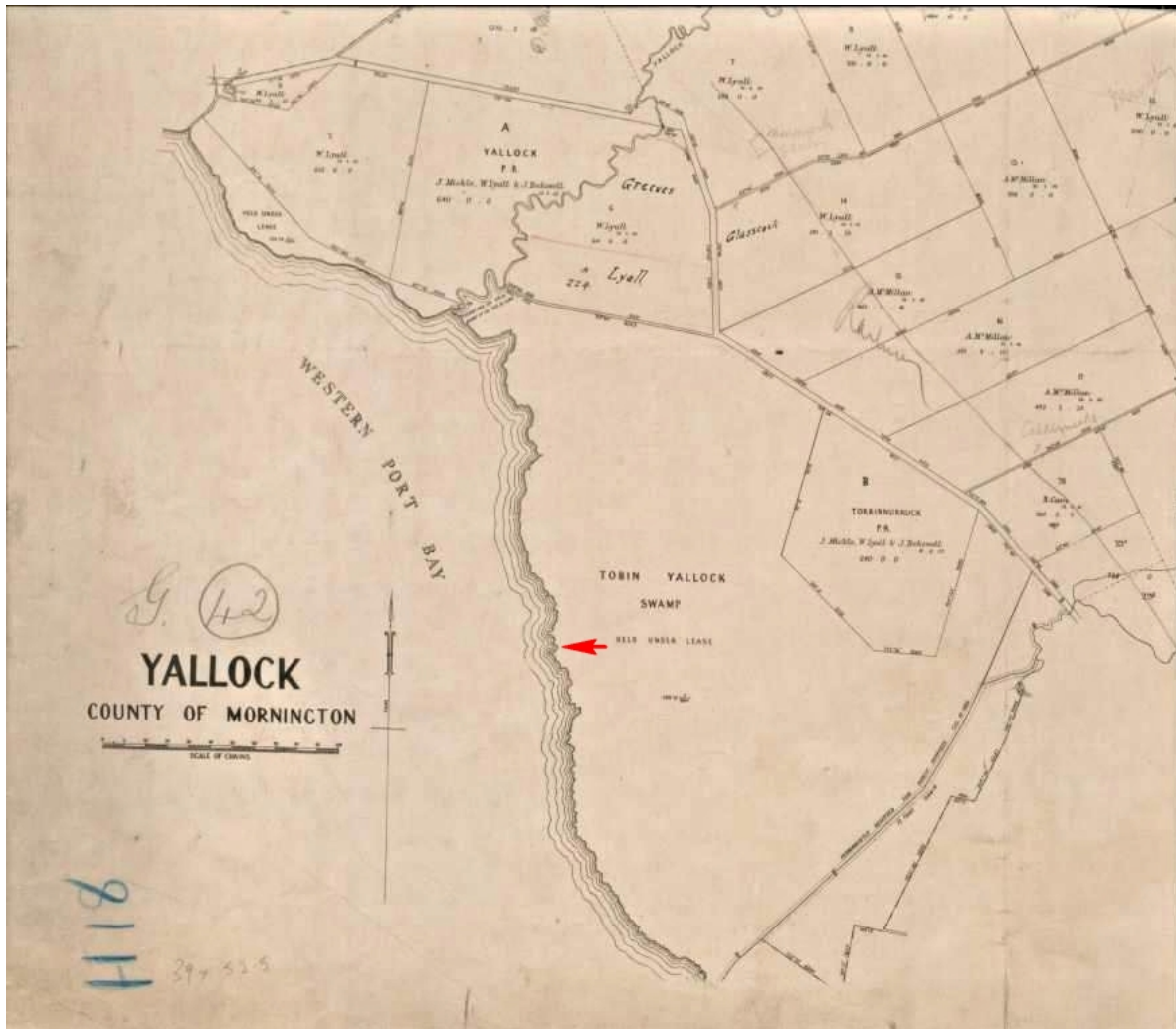


Figure 2. 1888 Department of Crown Lands and Survey Yallock Parish map, showing the Lang Lang River channel (bottom-right), Yallock Creek (top-centre) and a strongly crenulated coastline. The approximate location of the monitoring site is indicated by the red arrow.

2 Methods

2.1 DGPS and GPS field surveys of the Lang Lang coastline

Surveys of the coastline between the Yallock Drain and Lang Lang River channel were undertaken using a differential GPS (DGPS) and a hand-held GPS at the start and end of the monitoring period (25 October 2012 and 26 November 2013, respectively), to establish changes in the position of the banks over 12 months.

The GPS surveys covered the total length of the coastline from the drain to the river (8.6 km), which defined the study area within the ~11.5 km extent of the clay banks. The surveys were undertaken by setting the GPS (Garmin Dakota 20) to track recording at 1 second intervals and walking along the edge of the banks. The edge of the banks were defined as the uppermost break in slope, which was usually marked by a very distinctive, thin reddish unit overlying massive grey clays. The edge of the vegetation which tended to be stripped back from the banks was not considered to be the true edge of the banks (see Fig. 3). Surveying in the larger crenulations was problematic where the banks had been eroded to the sea wall, or covered by sand and shell deposits, or had been subject to bank revetment works. Hence, survey accuracy was poorer for approximately 1 km of the surveyed distance. This did not materially affect the long-term erosion estimates, which were based on averaging across multiple air photo periods in addition to the GPS survey.

The DGPS surveys covered approximately 4 km in several sections including the monitoring site in more detail. The original intention was to survey the entire length of the coastline using the DGPS, however, extremely boggy conditions at the time of the October 2012 field session, combined with the limited number of access points over the sea wall proved to be major limitations. A base station was set up over a temporary bench mark that was installed in the corner of the main paddock (UTM, 0368603, 5763073). The roving unit was used to survey the edge of the banks in detail as well as the location and heights of the monitoring equipment.



Figure 3. Typical bank profile where the vegetation and uppermost sediment has been stripped back from the bank edge exposing a distinctive thin reddish unit overlying massive grey clays. The true edge of the banks is indicated by the red arrow.

2.2 Aerial photograph interpretation

Air photo interpretation using historical air photos dating from 1947 was undertaken to calculate long-term erosion rates and examine any long-term changes in the shape of the coastline. The photos, sourced from the Victorian DSE, were selected according to a number of criteria including coverage, date, scale and resolution (Table 4). LIDAR DEM data (May 2008; 1 m resolution) was also obtained from Melbourne Water and used in the analysis.

Table 4. Air photos used to calculate long-term erosion rates and examine long-term changes in the shape of the shoreline.

YEAR	NAME	SCALE	COL/B&W	RUN	PHOTO
1947	n/a	1:15,840	B&W	1	104(?)
				2	47,49
				12	106
1970	Clyde Base Map project	1:12,000	B&W	14	251
1973	Western Port Project No. 1106	1:15,000	B&W	2	53
				3	45
				4	130
1977	Western Port Foreshores Project 1327	1:10,000	B&W	9	191,193,195,197,199,201,203
1984	Western Port Foreshores Project 1716	1:10,000	Colour	11	11,13,15,17,19,21
				10	194,196,198,200
1990	Melbourne Extension East Proj. 2034	1:15,000	Colour	41a	115

The photos were scanned and georectified in ArcMap 10.0 using the LIDAR DEM as a base map. The georectification process involved selecting as many known points as possible in the air photos relative to the DEM. Typical points included the junction of drains, roads and key points along the sea wall.

The outline of the coast was digitised using knowledge gained of the characteristics of the true edge to the banks (i.e. shape and colour) from the DGPS/GPS surveys. For the crenulations, the digitising followed the edge of the sand and shell deposits since the true edge of the banks was unknown. Consistency in approach was adopted so that the air photo analysis would be comparable, although it should be noted that there is likely to be a small degree of uncertainty in the results on the order of metres to 10's of metres.

On completion of the air photo interpretation, the results were compared to determine whether there were any major inconsistencies between the outlines that may be due to the georectification process. The main problem was slight differences in the alignment of photos since these could produce large errors in the results. On this basis, the 1970, 1973 and 1990 air photos were excluded and final analysis of the air photos was centred on the 1947, 1977 and 1984 photos, 2008 DEM, and the 2012 and 2013 DGPS/GPS surveys.

The GIS layers were used to determine the area and length of the coastline between the Yallock Drain and the Lang Lang River for each time-step. The data was then compared to calculate the area of sediment loss, average sediment yields, sinuosity (also known as the Crenulation Index) and average bank retreat rates. A visual assessment of the changes in the coastline over time was also made.

2.3 Selection of an erosion monitoring site

Field mapping of the banks along the Lang Lang coastline was undertaken to observe several key features including bank shape and orientation, as well as other important factors such as seepage and bioturbation. Field mapping was also used to guide the selection of a representative site where the bank erosion monitoring equipment would be installed. A number of criteria were used to select the site:

- Free of human modification including (concrete) revetment and sea walls;
- The range of bank shapes typical of the Lang Lang coastline, including steeply sloping, vertical, benched and faceted bank shapes;
- The range of erosional forms and geomorphic units typical of the Lang Lang coastline, including crenulated bays, headlands, a lower bench and tidal flats;
- Some depositional features, but not large areas of sand and shell deposits;
- Suitable for installing the monitoring equipment; and,
- Reasonable access by 4WD.

The site that was selected is ~ 800 m north of the main road/track access point to the coastline. It included a small crenulation and two headlands covering a distance of 175 m (UTM, 0368347, 5764251) (Fig. 4). The site was deemed to be representative of the Lang Lang coastline and hence would provide: i) reliable estimates of erosion rates that are transferable to other areas of the coastline, ii) a good understanding of the conditions during which erosion takes place, and iii) a good understanding of the erosion processes acting on all of the main geomorphic units.



Figure 4. View of the monitoring site at low tide looking north. In the image is a small crenulation with steeply sloping upper banks, a lower bench of ~ 0.5 m high, eroded material on the tidal flats (clay balls) and vertical-benched banks in the distance.

2.4 Installation of erosion pins and tape and clinometer surveys

One hundred 1 m stainless steel erosion pins were installed at the monitoring site to obtain point measurements of erosion over time (Fig. 5). The erosion pins were organised into 12 profiles (or transects), that extend around the crenulation and adjacent headlands. Between 7 and 10 pins were used per profile, positioned according to the geometry of the banks and pushed into the banks perpendicular to the surface. The first and last pins in the profile were positioned on the floodplain at the edge of the vegetation, and in the tidal flat, respectively. For these pins, 20 cm was left exposed. For all other pins, 10 cm was left exposed. All erosion pins were identified with stainless steel tags numbered from 0 to 100 and tied together with rope to prevent any losses. A tape and clinometer survey of the profiles was also undertaken to define the geometry of the banks and note the position and number of the erosion pins in each profile.

Re-measurement of the erosion pins was carried out at approximately 45-day intervals, dictated by the days when low tide occurred at around midday. This involved measuring the exposed length of each erosion pin to determine the cumulative amount of sediment lost over time, with the last measurement on 25 November 2013. Occasionally some of the pins were dislodged from the banks, especially those located on the lower bench. Where a pin was dislodged a maximum loss of 20 cm was assumed to be a reasonable estimate (although this could be an underestimate in some instances). The dislodged pins were repositioned back in the banks and subsequent losses were added to the previous total.

The tape and clinometer surveys were also repeated during each measurement to record the changes in bank geometry over time.



Figure 5. Example of one of the erosion pin transects, showing the geomorphic units identified. The units were also used to classify the heights reached during each high tide.

2.5 Installation of a monitoring camera and weather station

A solar-powered, remote 3G live-stream camera (Commando M-series HD 3.1 MP system) was installed at the southern end of the site (UTM, 0368334, 5764205) to remotely monitor and visually record changes over the 12 month period, particularly with respect to the impact of tides and storm events on erosion (Fig. 6). The lens was focused northwards to include the crenulation and headland banks in the distance of the image. Photographs of the monitoring site were captured at 15 minute intervals during daylight hours and automatically uploaded to a web platform which is accessed through the following link and login.

<http://csiocameras.com/view/>

Username: visitor

Password: Csiro

The camera images were analysed to determine changes in the banks over the 12 months. The images were also analysed to characterise the height reached during each high tide (using the classification shown in Fig. 5) and the prevailing wave conditions during each high tide (using the classification shown in Fig. 7).



Figure 6. Monitoring camera, solar panels and weather station installed at the site.



Figure 7. Examples of the classification system used to characterise the wave conditions during each high tide.

A Davis weather station was also installed with the camera, primarily to record wind speed and direction at the site (other variables such as temperature were also recorded as well). The data included 30-minute average wind speed and direction and, 30-minute maximum wind gust and direction for the site.

To establish longer-term, regional trends in wind patterns, records of wind speed and direction for the nearby stations of Rhyll (86373) and Cerberus (86361) were obtained from the Bureau of Meteorology. These datasets commenced in September 1991, providing 22 years of data. The three datasets were analysed to determine annual and seasonal trends in wind speed and direction, as well as wind conditions recorded during the periods between erosion pin measurements.

2.6 Installation of a groundwater piezometer and tide gauge

A groundwater piezometer was installed on the floodplain approximately 10 m from the edge of the banks (UTM 0368316, 5764349) to investigate groundwater levels and the role of pore water pressure in bank erosion. The piezometer incorporated a Schlumberger Cera-Diver data logger, positioned at 221.5 cm below the surface that was set to record average water pressure above the diver every 15 minutes based on 1 minute sampling intervals. A Schlumberger Baro-Diver was also installed to record atmospheric pressure every 15 minutes. Post-processing involved correcting the water pressure data with atmospheric pressure to determine the height of groundwater above the diver.

A Cera-Diver was also installed on the tidal flats between profiles 60 and 70 (UTM 0368322, 5764275) to record the tide heights at the site. The tide diver recorded average water pressure every 15 minutes based on 1 minute sampling intervals and was corrected with atmospheric pressure to determine the height of water in the bay above the diver.

During each field measurement, samples of bay-water and groundwater from the piezometer were obtained for measurement of electrical conductivity (EC) to calculate the density of the bay water and to obtain an approximate idea of the connectivity between the bay and groundwater. A similar EC is assumed to indicate direct connectivity between the water sources, whereas a lower EC in the groundwater is assumed to indicate inputs of fresh water from rainfall and catchment aquifers.

2.7 Sediment sampling and laboratory analysis

A bank exposure at the monitoring site was analysed to characterise the sedimentary layers and obtain samples for laboratory analysis (Fig. 8). In-situ coring was also undertaken to provide additional stratigraphically-intact samples, however, the coring had poor results. Core retrieval proved unsuccessful for a number of cores with the sediment failing to stay in the core barrel, whereas the retrieved cores were compressed both through hammering the corer into the ground and removing the core from the barrel. No deep cores (≥ 2 m) were successfully retrieved.

Laboratory analysis of the samples was undertaken to determine the sedimentological properties of the bank material. Bulk density (mass of soil per unit bulk volume), porosity (volume of pores (or voids) in the soil relative to the total volume of soil) and saturation (the proportion of soil pores filled with water relative to the total pores) were determined by collecting samples using a bulk density ring of known volume. The samples were weighed, oven dried at 105 °C for 122 hours and re-weighed. The following equations were used to calculate the results:

$$Pb_{(dry)} = \frac{Ms_{(dry)}}{V} \quad (i)$$

$$Pb_{(moist)} = \frac{Ms_{(moist)}}{V} \quad (ii)$$

$$\% moisture = \frac{Ms_{(moist)} - Ms_{(dry)}}{Ms_{(moist)}} \times 100 \quad (iii)$$

$$\% \phi = 1 - \frac{Pb_{(dry)}}{Ps} \times 100 \quad (iv)$$

$$\% S = \frac{V_w}{\phi} \times 100 \quad (v)$$

$$V_w = \frac{Ms_{(moist)} - Ms_{(dry)}}{V\rho_w} \quad (vi)$$

Where Pb_{dry} is the density of dry soil ($g\ cm^{-3}$), $Pb_{(moist)}$ is the density of moist soil ($g\ cm^{-3}$), $Ms_{(dry)}$ is the mass of dry soil (g), $Ms_{(moist)}$ is the mass of moist soil (g), V is the volume of the cylinder used in sampling (cm^3), ϕ is porosity (%), Ps is the particle density ($g\ cm^{-3}$), V_w is the volumetric water content, S is saturation and ρ_w is the density of water ($g\ cm^{-3}$). A clay particle density of $2.65\ g\ cm^{-3}$ was assumed, except for layer 4 (183-200 cm) which had a higher organic matter so a clay particle density of $2\ g\ cm^{-3}$ was used. The density of water in the bay was calculated as $1.0216\ g\ cm^{-3}$, recognising that this is also temperature dependent.

Sediment dispersion was analysed using the Emerson Aggregate Test. This involved placing two small air dried aggregates into a beaker of 50 mL distilled water and observing the degree of dispersion, slaking and swelling after 2 hours and 20 hours. Organic matter content was determined by measuring total organic carbon. Air dried subsamples of the soils were crushed to $< 2\ mm$ and treated with acid to remove the inorganic carbon, then fired in a Leco Furnace at $>550\ ^\circ C$ for 3 minutes. Particle size analysis (i.e. percent clay:silt:sand) was undertaken using the hydrometer method. Air dried, crushed and dispersed subsamples were placed in a 1 litre cylinder with distilled and the density of the solution was measured at 5, 30, 93 and 420 minutes using a hydrometer. The soil sample measurements were corrected with hydrometer readings from a 1 litre blank solution consisting of distilled water and Calgon. The sand fraction in each soil sample was sieved to measure the proportion of fine (0.02-0.2 mm) and coarse ($> 0.2\ mm$) sand. Soil texture was determined from particle size. pH and EC were measured by mixing a subsample of air dried soil with water to form a 1:5 ratio, tumbling for 1 hour, then measuring with pH and EC meters.



Figure 8. Left: Bank profile sampled at the monitoring site showing 4 of the 5 sedimentary layers and prominent surface cracking. Right: Bank profile near the Lang Lang River, with a large piece of buried wood marking the boundary between a red-brown organic-rich clay layer and the lowermost grey clay unit.

2.8 Fetch and wave modelling

An analysis of fetch across the bay (the longest unobstructed distance over water in a constant direction) was undertaken to explore the impact on wind-generated wave heights (i.e. a longer fetch can result in larger waves). Fetch was calculated using the USGS Wind Fetch Model which is run in ArcGIS 10.1 (Rohweder *et al.*, 2012).

The input data into the model included a 1-second Shuttle Radar Topographic Mission (SRTM) DEM, which was used to define the land boundary around the bay (28 m pixel size). The western and eastern entrances to the bay were clipped and a 'land' value was applied to remove the impacts of having an 'unbounded' fetch in the model. Hence for these areas, the results are an underestimate.

Wind direction was specified in the model at 22.5° intervals (i.e. N, NNE, NE, ENE, etc). The model offers 3 methods of calculation: SPM (Shore Protection Manual), SPM-restricted and single, of which the default SPM method was used since it takes into account the problem that wind direction is rarely static. The method first, determines the fetch for 9 radials at 3° intervals distributed evenly on either side of each specified wind direction (e.g. 78°, 81°, 84°, 87°, 90°, 93°, 96°, 99°, 102°), and second, calculates the arithmetic mean of the 9 radials to provide a fetch value that is relatively representative of the real-world situation.

The outputs from the model (i.e. fetch for each wind direction) were analysed to determine seasonal trends, relative to the seasonal wind direction patterns determined from the monitoring site, Cerberus and Rhyll wind data.

Simple wave modelling was undertaken using the USGS Wave Model in ArcGIS 10.1 to simulate wind-wave heights across the bay based on the observed wind data at the monitoring site. The model has a number of assumptions and limitations. For example, it uses simplistic methods to calculate wave parameters, the algorithms are based on a deep-water model which does not consider the impact of

friction from the bed surface (meaning that wave heights will be slightly over-estimated) and, the model does not account for wave refraction or interactions (Rohweder *et al.*, 2012). The model also assumes that the water depth is constant (i.e. non-tidal conditions). Nonetheless, it was considered useful for our purposes to gain an idea of the impacts of the differences in fetch and wind speed on wind-wave heights across the bay for a maximum water level and to gain an idea of the *relative* differences in wave power between various sites around the bay.

The model input data includes the 1-sec DEM, 1 m bathymetry DEM obtained from Melbourne Water, fetch layers derived from the Wind Fetch Model and the observed wind speed and direction data for average winds and maximum gusts from the monitoring site (simulation period: 2 Nov 2012 to 11 Nov 2013). To reduce the number of model outputs to a manageable level, the wind data was binned into the following categories: All wind directions (16) – 10, 20, 30, 40, 50 km hr⁻¹; All westerly wind directions from N to S (i.e. N, NNW...SSW, S) (9) – 60, 70, 80, 90, 100 km hr⁻¹. Data was assigned to a bin using the following criteria: bin wind speed ± 5 km hr⁻¹ (e.g. 10 km hr⁻¹ bin includes winds 5-15 km hr⁻¹). The height of the anemometer was specified as 3.5 m above the ground surface, while water density was 1021.6 kg m⁻³.

The Wave Model generates rasters that span the geographical extent of the bay for the wave variables selected; in this study the selected variable was wave height. The data was extracted using the coordinates for 3 sites: the monitoring site, Grantville and Jam Jerrup, noting that other sites around the bay could also be analysed in the future.

The modelled wave height data was used to calculate wave energy using equation (vii) below. The recorded water depth from the tide diver installed at the monitoring site was used to calculate wave speed using equation (viii) (shallow water equation). The calculated wave energy and wave speed was used to estimate wave power (equation ix), where wave power is the rate at which energy is supplied at a location such as a beach or banks. It should be noted that the water power equation does not take into account the shape of the banks and whether there is a long or short run-up. The slope and length of the run-up has an important effect on the transfer of kinetic energy at the bank surface, and hence should be considered in further modelling work.

$$E = \frac{\rho g H^2}{8} \quad (\text{vii})$$

$$C = \sqrt{gd} \quad (\text{viii})$$

$$P = EC \quad (\text{ix})$$

Where E is water energy per unit area of a wave (J m⁻²), ρ is water density (kg m⁻³), g is gravity (m s⁻¹), H is wave height (m), C is shallow water wave speed (m s⁻¹), d is water depth (m) and P is wave power (kW per meter length of wave crest).

3 Results

3.1 Morphology and sedimentology of the banks

The morphology of the banks along the Lang Lang coastline are similar to those described in a generic classification of bank slope by Crouch (1987) (see Fig. 9). Hence, this classification has been adopted here. Most of the banks at Lang Lang are either benched or vertical, although steeply sloping and faceted banks feature regularly as well (Fig. 10). The benched and sloping banks are widely distributed along the length of the coastline whereas vertical banks seem to occur where the banks are south or south-west facing. Some of the upper parts of the vertical banks show slight undercutting or a wave-cut notch of ~ 10 cms. But only occasionally has the undercutting resulted in collapse of the material above by toppling. Facetted banks are more prominent in the central, highly crenulated area immediately south of the monitoring site. This shape also seems to be characteristic of many of the headlands in this area. No evidence of bank slumping (rotational failure) was observed along the coastline examined.

Where the banks have a benched morphology, the benching occurs in the lower ~ 0.5 m of the banks and is an erosional, rather than depositional feature. The bench usually extends for tens of meters from the bank crest in the crenulations, and a lesser distance at the headlands. The bench is not a continuous feature along the coastline, although it does occur at a similar height, and appears to be the result of a structural and sedimentological control in the bank material. Facetted banks also appear to reflect structural and sedimentological controls.

Along most of the banks the vegetation and ~ 30 -40 cm of silty clay sediment has been stripped off by about 2-3 m to reveal a distinctive edge or bank crest which is clearly marked by a reddish sedimentary unit. There are few areas where the vegetation extends to the edge of the banks, but in these areas the vegetation is usually not continuous. Instead the upper sediment and vegetation have been stripped back to form a scalloped pattern. This stripping effect also appears to be the result of a structural and sedimentological control.

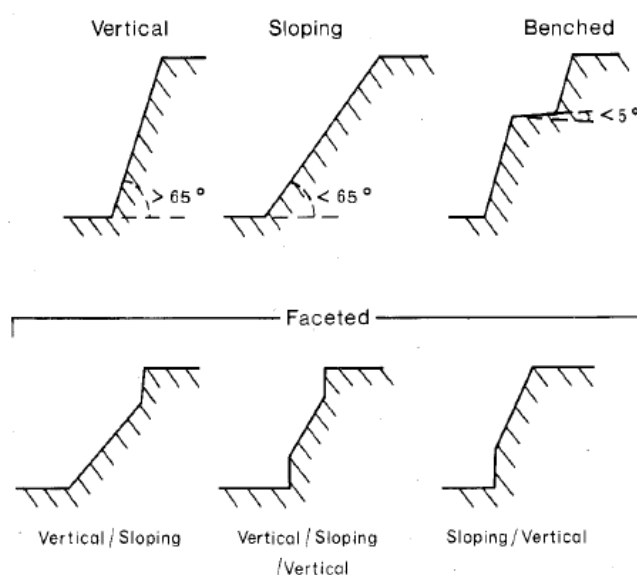


Figure 9. Generic classification of bank slope profiles (Source: Crouch, 1987).



Figure 10. Classification of bank profiles between the Yallock Drain and the Lang Lang River.

The sedimentology of the bank material can be characterised into five layers that are laterally continuous along the length of the Lang Lang coastline (Table 5). The sedimentology appears to have a strong influence on the morphology of the banks with changes in the shape of the banks (and geomorphic unit), coinciding with changes in the sedimentology. The uppermost unit which characterises the floodplain (and sediment stripped from the edge of the banks) consists of horizontally laminated brown silty clays. This is underlain by a thin (7 cm) reddish silty clay layer which tends to demarcate the crest of the banks. The upper and lower banks are composed of cohesive, massive grey clays. There is no obvious boundary within the grey clays probably due to the effects of bioturbation by crabs and polychaetes. However, the sedimentology suggests that there are some differences, with the lower bank material being finer and more stable, while the upper bank material is slightly coarser and more dispersible.

The bench surface is characterised by a thin (17 cm) silty loam layer which has abundant, well preserved leaf and wood material including remnant stumps of trees. This layer appears to represent an older swamp surface that was subsequently buried by the overlying clays and silty clays. Material forming the bench face is composed of grey silty clays and a key feature of this layer is the many holes which act to increase the surface area for erosion. Many of these holes are likely to have been formed by crabs and through the decomposition of old roots. The bench face layer appears to extend deeper, and potentially forms the main substrate comprising the tidal flats, which is subsequently blanketed by a veneer of fine suspended sediment.

Despite the high clay and silt content (weighted average of 77 % compared to 17 % sand and 6 % organic matter), all of the sedimentary layers have a relatively low dry bulk density, high porosity and high saturation indicating that the sediments are uncompacted and pervious. The lowest dry bulk density and highest porosity and saturation occurred in the bench surface material due to the relatively high proportion of undecomposed organic matter. Bioturbation is also likely to be playing a significant role in maintaining the porosity of the sediments, particularly through the construction of tunnels and holes.

There is a small difference in the dispersibility of the layers with the lowest layers remaining stable after 2 and 20 hours, while the upper layers show some dispersibility. However, the degree of dispersibility is probably not significant given that the typical duration of high tide is on the order of a few hours or less. No significant swelling of the samples was observed in the laboratory analysis, however, cracking and shrinking of the upper few centimetres of surface sediment in the red silty clay layer and grey clays was observed in the field relating to wet and drying of the surface over the tidal cycle.

The sedimentology and morphology of the banks suggests that erosion is occurring through physical processes such as abrasion and plucking of surface sediment, rather than chemical processes like dispersion, or failure of the banks through rotational slumping. The stability and high clay content of the bank sediments implies that they are relatively resistant to erosion, with some differences between the upper and lower layers relating to particle size, cohesion, degree of bioturbation and organic matter. The most resistant layer appears to be the bench surface and this is clearly playing a role in protecting the underlying sediment, while the least resistant layer is the floodplain which is in part protected by the vegetation. The resistance of the middle grey clay unit is in between. Based on the sedimentology, the banks at Lang Lang have a low erosional susceptibility, however daily wave attack during the tidal cycle is clearly a major factor in counteracting erosion resistance.

Table 5. Sedimentology of the bank material.

DEPTH (CM)	GEOMORPHIC UNIT	FIELD DESCRIPTION AND BOUNDARY	SAMPLE DEPTH (CM)	PH	EC (MS CM ⁻³)	MOISTURE (%)	BULK DENSITY (G CM ⁻³ / T M ⁻³)		POROSITY (%)	SATURATION (%)	DISPERSION		PARTICLE SIZE				SOIL TEXTURE (DETERMINED FROM PARTICLE SIZE)
							Moist	Dry			2 hrs	20 hrs	Clay (%)	Silt (%)	Sand ^a (%)	OM ^b (%)	
0-39	Floodplain	Horizontally laminated brown clay with fine fibrous roots Clear	25	6.58	4.29	45.4	1.32	0.72	72.8	81.1	Stable	Slight dispersion 1	47.5	22.5	24.1	5.9	Silty clay
39-46	Bank crest	Thin reddish boundary layer composed of clay pellets Clear	42	6.90	4.86	42.8	1.50	0.86	67.5	93.3	Slight dispersion 1 and possible slaking	Dispersed 2	57.5	20.0	17.2	5.3	Silty clay
46-183	Upper and lower banks	Massive grey clays with active bioturbation (polychaetes and crabs) Diffuse	60	6.91	4.44	44.6	1.49	0.82	68.9	94.1	Very slight dispersion	Dispersed 2	65.0	17.5	13.6	3.9	Clay
			150	6.43	5.99	51.3	1.42	0.69	73.9	96.7	Stable	Slight slaking	72.5	12.5	9.7	5.3	Clay
183-200	Bench surface	Red-brown clay with abundant fibrous organics (leaves) and wood Diffuse	191	5.66	8.11	78.3	1.11	0.24	88.0	96.8	Stable	Stable	20.0	14.3	42.6	23.1	Silty loam, with high organic matter
200-	Bench face	Massive grey	225	6.38	7.03	62.4	1.28	0.49	81.8	95.6	Stable	Stable	55.0	22.5	16.6	5.9	Silty clay

DEPTH (CM)	GEOMORPHIC UNIT	FIELD DESCRIPTION AND	SAMPLE DEPTH (CM)	PH	EC (MS CM ⁻¹)	MOISTURE (%)	BULK DENSITY (G CM ⁻³ / T M ⁻³)	POROSITY (%)	SATURATION (%)	DISPERSION	PARTICLE SIZE				SOIL TEXTURE (DETERMINED FROM PARTICLE		
250+		clays with sporadic roots and many holes															
Weighted average for bank profile				6.53	5.62	52.4	1.38	0.66	74.7	93.2	-	-	59.1	17.8	16.8	6.4	-

^aMost of the sand fraction is very fine to fine sand (63-250 µm)

^bOM: Organic matter

3.2 Long-term estimates of bank erosion rates using aerial photographs, GPS surveys and LIDAR

Analysis of the 1947, 1977 and 1984 air photos, combined with the 2008 DEM, and the 2012 and 2013 GPS surveys of the site revealed that there have been some clear changes in the position of the edge of the banks over time (Figs 11 & 12). There has been progressive horizontal retreat of the banks resulting in a total area of sediment loss of 232,923 m², or 270 kt, over 65 years between the Yallock Drain and the Lang Lang River (Table 6). This equates to an average area of 3583 ± 2479 m² yr⁻¹ and an average sediment yield of 4.2 ± 2.9 kt yr⁻¹ from the 8.6 km stretch of coastline, which is within the lower range of previous estimates.

The air photo records show that erosion of the coastline has not been spatially and temporally uniform over time. There is clear evidence that the headlands and crenulations have become less pronounced since 1947 particularly in the area marked A on Fig 11. Most of the increased erosion of the headlands seems to have occurred between 1947 and 1977 and this is confirmed by calculations of the sinuosity of the coastline. Sinuosity decreased from 1.37 to 1.27 between 1947 and 1977 (Table 6) and has only slightly decreased since 1977. The sinuosities calculated for the 2012 and 2013 GPS surveys are marginally higher, but these probably reflect the more detailed survey of the coastline, rather than a true increase in length. It is unknown whether the sinuosity of the coastline was greater prior to 1947. The 1888 parish map (Fig. 2) suggests that the coastline was considerably more crenulated compared to the 1947 air photos, so it is likely that sinuosity was higher and has been decreasing over a long period of time, possibly reaching an equilibrium in the last 30 years or so.

There are also some areas that appear to have experienced consistently greater or lesser erosion relative to other sections of the banks. The areas with greater erosion include those banks near the drain outlets (marked B) and some of the very large crenulations (marked C). In many of these areas, bank erosion of the order of 30-50 m has reached or even surpassed the sea wall resulting in its reconstruction and realignment further inland. In the last few decades there have been several efforts to try to reduce erosion of the sea wall by using rock (concrete) revetment so it is likely that erosion of these areas could have extended further under natural conditions. There also seems to be a trend for greater bank erosion (> 20 m) on the north-west facing sides of the crenulations compared with lesser erosion (< 20 m) on the south-west facing sides. This observation does not hold true for the entire length of the coastline, including the monitoring site (Fig. 12), but it is frequent enough along the coastline to warrant comment here.

There is clear evidence that the rates of erosion vary over time at least on decadal to multi-decadal timescales, and potentially on an annual to sub-decadal timescale. Average bank retreat rates from the air photos range from 0.29 m yr⁻¹ to 0.96 m yr⁻¹, with a long-term average rate of 0.42 ± 0.29 m yr⁻¹ over the 65 years (Table 6). The highest rates of erosion occurred between 1977 and 1984. However, these higher rates may be a reflection of the shorter time period between photos since longer periods tend to give lower rates due to the greater potential to average out the highs and lows. Nonetheless, it is likely that there have been periods of higher erosion prior to 1977 and after 1984, with maximum bank erosion rates potentially equalling or exceeding 1 m yr⁻¹.

The magnitude and variability in average bank retreat rates and sediment yields determined in this study is consistent with the previous work by Hurst (2012) using aerial photographs from 1973, 1984 and 1996, and 2009 satellite imagery. However, our estimates of average sediment yields are higher than previous estimates by Sargeant (1977), but lower than reports by Wallbrink *et al.* (2003) and Hurst (2012). One of the main differences in calculating sediment yields is the length of the coastline examined. In our study, sediment yields were calculated for the coastline between Yallock Drain and the Lang Lang River (8.6 km) (since this was the distance covered by the GPS survey and therefore

the limiting factor in the comparison with the air photos). Another difference is the bulk density used to convert the area of sediment loss into yield. The Wallbrink *et al.* and Hurst studies assumed a bulk density of 1.5 t m^{-3} which is a typical value for sandy soils. Whereas, our analysis of the sedimentology of the site indicates that a value of 0.6645 t m^{-3} is more appropriate. A third difference is in the height of the banks. We calculate an average height of 1.74 m from the DEM (including the crenulations) whereas Hurst assumes an average height of 2.2 m. Further differences arise due the different methods used to estimate sediment loss (e.g. sediment tracers vs GIS analysis of air photos), differences in the magnitude of errors associated with those methods and differences in the timeframe considered since erosion appears to vary spatially *and* temporally.

When adjusted for length, bulk density and height, Hursts' results equate to an average sediment yield of 4.9 kt yr^{-1} . When adjusted for bulk density (assuming a similar bank height and coast length), the results from Wallbrink *et al.* equate to a sediment yield of 8.9 kt yr^{-1} . Both of these adjusted yields are within the range reported here (i.e. min of 2.9 kt yr^{-1} to max of 9.4 kt yr^{-1}). However, it is also clear from the data that in some years sediment yields from erosion of the banks at Lang Lang have been in the order of 10 kt yr^{-1} and possibly higher.

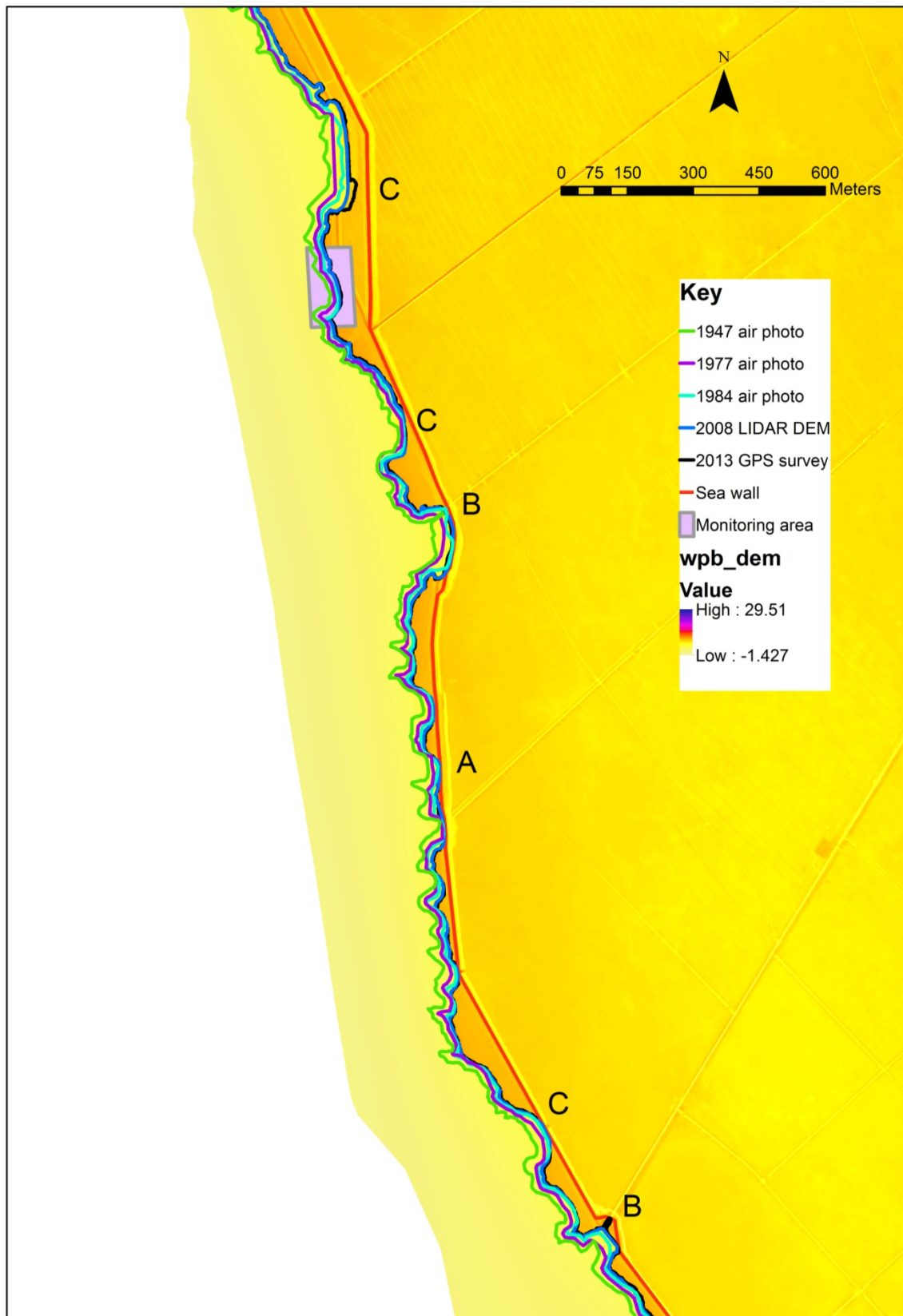


Figure 11. Snap-shot of the historical air photo analysis showing the smoothing of the headlands and retreat of the banks over time. Labels are as follows: 'A' indicates the general area where there has been pronounced smoothing of headlands and crenulations over time; 'B' indicates areas of enhanced erosion due to the drain outlets; 'C' indicates the very large crenulations which are, or have in the past, threatened the sea wall. The air photo mapping indicates the position of the upper edge of the banks.

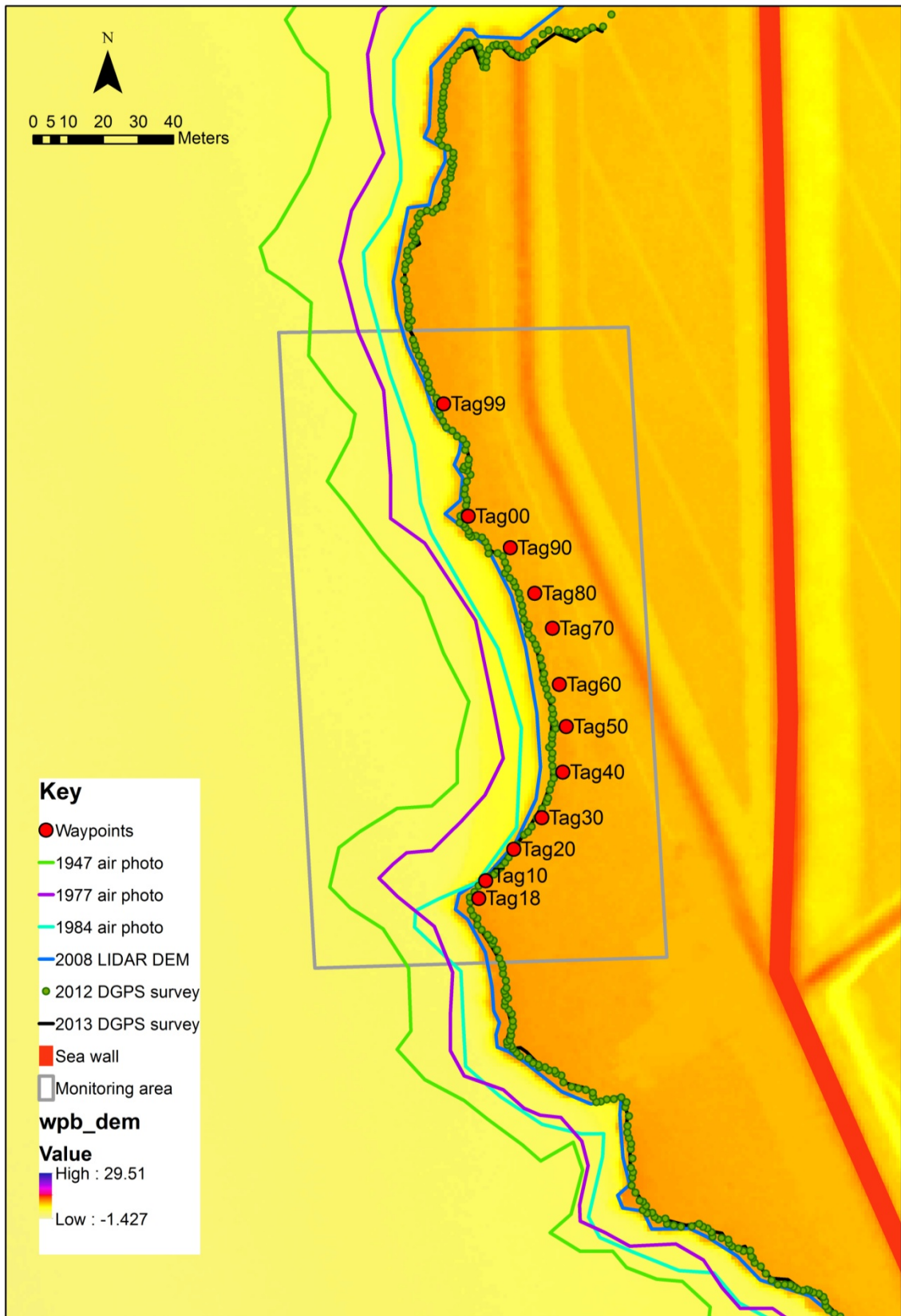


Figure 12. Change in the position of the upper edge of the banks at the monitoring site between 1947, 1977, 1984, 2008, 2012 and 2013. The location of the first pin in each erosion pin profile is also shown.

Table 6. Long-term rates of sediment loss and sediment yield between the Yallock Drain and Lang Lang River.

	GIS POLYGON AREA (M ²)	AREA OF SEDIMENT LOSS ^a (M ²)	NO. OF YEARS	AVERAGE AREA OF SEDIMENT LOSS (M ² YR ⁻¹)	AVERAGE SEDIMENT YIELD ^b (KT YR ⁻¹)	GIS POLYGON PERIMETER (M)	COAST LENGTH ^c (M)	DIFFERENCE IN COAST LENGTH (M)	CRENULATION INDEX OR SINUOSITY ^d	AVERAGE BANK RETREAT ^e (M YR ⁻¹)
1947 air photo	19,858,343	-	-	-	-	24,216	9071	-	1.37	-
1977 air photo	19,758,037	100,305	30	3344	3.9	23,495	8389	-682	1.27	0.40
1984 air photo	19,701,437	56,601	7	8086	9.4	23,519	8428	38.9	1.27	0.96
2008 DEM	19,642,732	58,705	24	2446	2.8	23,404	8340	-87.7	1.26	0.29
2012 GPS survey	19,625,419	17,313	4	4328	5.0	23,650	8580	240.3	1.29	0.50
2013 GPS survey	19,626,635	(+1,216 ^f)	1	n/a	n/a	23,539	8517	-63.2	1.28	n/a
Total (1947-2012)	-	232,923	65	-	-	-	-	-	-	-
Long-term average	-	-	-	3583	4.2	-	8562	-	1.29	0.42
Standard deviation (1σ)	-	-	-	2479	2.9	-	298.4	-	0.05	0.29

^aCalculated as the difference in polygon area from previous.

^bCalculated using an average bank height of 1.74 m determined by GIS using the 2008 DEM and a sediment bulk density of 0.6645 t m⁻³ determined from the dry bulk density and thickness of each sedimentary layer (i.e. weighted average), shown in Table 5.

^cCalculated by subtracting the non-coastal part of the polygon perimeter from the total perimeter.

^dCalculated as the actual coast length divided by the straight line distance (6630 m).

^eCalculated as the average area of sediment loss divided by the coast length.

^fThe gain in sediment is not a true gain but rather a reflection of errors in the GPS surveys (e.g. errors in satellite positioning and signal reflectance)

3.3 Bank erosion rates during the monitoring period: November 2012 to November 2013

Since installation of the erosion pins on 30 October 2012, the cumulative average sediment loss across all profiles at the monitoring site to 25 November 2013 was 33.2 cm (Fig. 13, Table 7). When extrapolated, this equates to an average loss of ~ 1 mm day⁻¹ or 2.6 cm month⁻¹ or 0.31 m yr⁻¹. There is some monthly variability in the rates of erosion measured, ranging from 1.47 to 3.73 cm mth⁻¹, with the lowest erosion recorded from May to August, and the highest erosion occurring in April and September-mid October.

On a smaller spatial scale, the amount of sediment loss by profile varied considerably over the 12 months (Fig. 14). The profiles with the highest average losses (greater than the 33.2 cm average) were 18, 10, 00 and 99. Profile 00 on the northern headland recorded the maximum average loss of 65.9 cm over the 12 months followed by profile 18 on the southern headland which recorded 53.8 cm of sediment loss. However it should be noted that these profiles also experienced the most number of pins dislodged, particularly for the July, August and October measurements, so the figures may be an under- (or over-) estimate of the true erosion that occurred. In contrast, the profiles with the lowest average losses were 50, 60 and 70, which are located at the apex of the crenulations, while the minimum total average erosion recorded was 19.5 cm at profile 60.

The amount of sediment loss for each erosion pin also varied substantially. Maximum cumulative losses of greater than 1 m were recorded at seven erosion pins located on the bench face (to a maximum of -146.2 cm) and one erosion pin in the upper banks (-109.2 cm). Many of these pins were dislodged over the 12 months indicating that the losses could have been much higher. For several pins located on the floodplain, lower banks, bench surface and tidal flats, deposition of sediment up to 7.5 cm was recorded over the 12 months.

Similar patterns are revealed when the results are analysed by geomorphic unit (Table 8). The greatest erosion (53.5-146.2 cm) occurred on the bench face, followed by the upper banks, then lower banks and bank crest, noting that there were significant differences in the amounts of sediment loss between profiles. The geomorphic units with the least erosion and/or deposition, were the floodplain and bench surface, excepting profiles 18, 10 and 00. The tidal flats also showed continuous fluctuations between deposition and erosion within ± 10 cm. Sediment deposits were typically characterised by sand, shells and mud similar to that shown in Fig. 13.

The patterns of erosion recorded by the erosion pins are clearly reflected in the tape and clinometer surveys of the profiles (Fig. 15). The steeper sub-vertical parts of the banks (i.e. upper and lower banks and bench face) show the greatest erosion. They also show that erosion is occurring by parallel retreat of the bank face. Conversely, the near-horizontal surfaces (i.e. floodplain, bench surface and tidal flats) show very little downward erosion over the 12 months. The bench surface creates a (relatively) long wave run-up, especially for profiles 30 to 80, which may have an influence on the rate of erosion of the lower and upper banks, crest and floodplain in these profiles.

The results from the erosion pins were very consistent with those from the air photo analysis, providing confidence in our results. For instance, the average erosion rate of 0.31 m yr⁻¹ calculated for the monitoring site is similar to the long-term average erosion rate of 0.42 m yr⁻¹ and is within the minimum-maximum range of 0.29-0.96 m yr⁻¹. The calculated sediment yields for the monitoring site are slightly higher with an average of 6.2 kt yr⁻¹, but this is largely due to differences in the calculation of erodible area. Nonetheless, the estimated sediment yields based on the erosion pin transects are within the long-term range of 3-10 kt yr⁻¹. The observations from the air photos of faster erosion of the headlands were also measured at the monitoring site. While the apex of the crenulation which recorded the least erosion over the 12 months is also consistent with the longer term trends identified from the air photos.

The remaining questions are the persistence of these trends and the longevity of the crenulations and the bench, relative to the headlands. The early historical accounts describe rills of freshwater flowing from the Tobin Yallock Swamp (Table 3) and it is possible that these rills were a key factor in maintaining the crenulated form of the coastline. Today, anthropogenic modifications are impacting on the shape of the

coastline including the drain outlets which amplify local erosion and the concrete revetment walls which decrease local erosion.



Figure 13. Erosion monitoring site showing the edge of the banks (jagged black line) and edge of the lower bench (light blue line) as surveyed in October 2012. The location of the first erosion pin in each profile, camera, groundwater piezometer, tide gauge and bank profile analysed are also shown. The image in the background is a 2008-9 air photo which shows some sand deposition on the bench surface and floodplain at the centre of the crenulation. The air photo also shows the position of the edge of the bench and top of the banks in 2008-9. The length of the coastline from BankProfile to Tag18 is 175 m.

Table 7. Average rates of sediment loss measured from the erosion pins over the 12 months (392 days) of monitoring.

DATE OF MEASUREMENT	DAYS SINCE LAST EROSION PIN MEASUREMENT	CUMULATIVE SEDIMENT LOSS (AVERAGE OF ALL PROFILES) (CM)	DIFFERENCE FROM PREVIOUS (CM)	SEDIMENT LOSS PER DAY (CM)	EXTRAPOLATED SEDIMENT LOSS PER MONTH (CM)	EXTRAPOLATED SEDIMENT LOSS PER YEAR (CM)	ESTIMATED SEDIMENT YIELD (KT YR ⁻¹) ^A
30-Oct-12	0	0	-	-	-	-	-
18-Dec-12	49	-4.833	-4.833	-0.101	-3.121	-36.7	7.2
4-Feb-13	48	-9.453	-4.621	-0.096	-2.984	-35.1	7.1
20-Mar-13	44	-13.162	-3.709	-0.084	-2.613	-30.8	6.2
23-Apr-13	34	-17.118	-3.956	-0.116	-3.607	-42.5	8.5
3-June-13	41	-19.267	-2.150	-0.052	-1.625	-19.1	3.8
17-July-13	44	-21.35	-2.08	-0.047	-1.466	-17.3	3.5
28-Aug-13	42	-24.03	-2.68	-0.064	-1.977	-23.3	4.7
14-Oct-13	47	-29.68	-5.66	-0.120	-3.730	-43.9	8.8
25-Nov-13	43	-33.161	-3.48	-0.081	-2.508	-29.5	5.9
Average	43.6	-	-3.685	-0.084	-2.619	-30.8	6.2

^aCalculated using the sediment loss per year, a bulk density of 0.6645 t m⁻³ and an estimated bank area of 30,196 m² determined using GIS and the 2008 DEM.

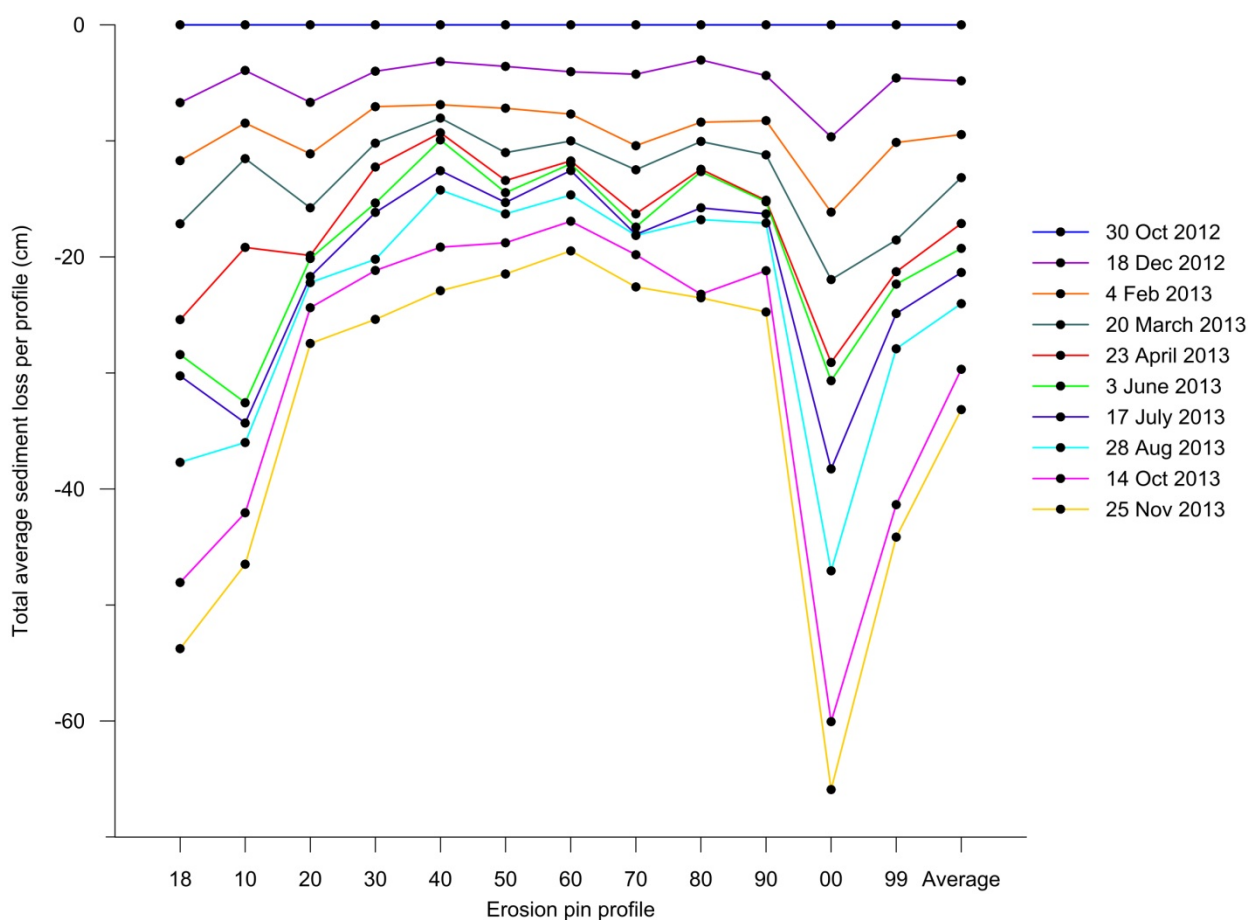


Figure 14. Total average sediment loss per erosion pin profile since the start of monitoring.

Table 8. Variability in erosion by geomorphic unit. Erosion is indicated by negative values, while deposition is indicated by positive values.

GEOMORPHIC UNIT	RANGE OF EROSION MEASURED (CM, CUMULATIVE WITH EACH COLLECTION)	PROFILES WITH THE HIGHEST EROSION	PROFILES WITH THE LOWEST EROSION
18 December 2012 (49 days of monitoring)			
Floodplain	0 to -3.5	60,70,00	10,20,40,99
Bank crest	-0.1 to -5.4, to max -20.3	00,18	10,20,40,50
Upper banks	-0.9 to -10.5	00,18,99	40-60
Lower banks	-3.4 to -12.8	90,00	30,40
Bench surface	+5.3 to -4.4	18,10,99	20-00
Bench face	-10.7 to -39.4	18,20,90,00,99	10,40,70
Tidal flat	+2.8 to -4.2	18-40	80,90,00
4 February 2013 (97 days of monitoring)			
Floodplain	0 to -6.4	00,18	10-90,99
Bank crest	-0.5 to -8.8, to max -31.7	00,18	50
Upper banks	-3.6 to -19.6	18,10,90,00,99	30-70
Lower banks	+5.1; -6 to -19.8	60-90,00,99	18-50
Bench surface	-0.5 to -9.4	18,10,90,00,99,60	20-50
Bench face	-19.8 to -39.6	18,99	30
Tidal flat	+4.6 to -7.1	20-80	18,10,90,00,99
20 March 2013 (141 days of monitoring)			
Floodplain	+1.3 to -8	00,18	All except 00 & 18
Bank crest	-1.5 to -18.6, to max -39	00,18	10,40,60,80,90
Upper banks	-6.2 to -27.2	90,00,99,18,10	30-70
Lower banks	+2.1 to -27.5	10,20,50,60,80,90,00,99	Variable
Bench surface	-0.9 to -9.7	18,10,60,70,90,00,99	30-50
Bench face	-28.5 to -65	99,00,20,70,50	18.40,80
Tidal flat	+4.2 to -6.6	30-70	18,10,99
23 April 2013 (175 days of monitoring)			
Floodplain	+2.4 to -11.4	00,18	All except 00 & 18
Bank crest	-1.8 to -45	00,18,10	40,60-90
Upper banks	-9.6 to -31.1	18,10,70,90,00,99	30-70
Lower banks	-4.1 to -30	00,80,50	Variable
Bench surface	-1 to -10.2; max -35.5	18,20,70,99	30-60, 80
Bench face	-29 to -81.5	18,10,00	20-50
Tidal flat	+3 to -5.6	18,20-70	99,00
3 June 2013 (216 days of monitoring)			

GEOMORPHIC UNIT	RANGE OF EROSION MEASURED (CM, CUMULATIVE WITH EACH COLLECTION)	PROFILES WITH THE HIGHEST EROSION	PROFILES WITH THE LOWEST EROSION
Floodplain	+2 to -12.4	00	All except 00 & 18
Bank crest	-2 to -47.7	00,18,10	40, 60-90
Upper banks	-9.6 to -32.6	18,10,70,90,00,99	30-70
Lower banks	-3.3 to -29.9	50,00	Variable
Bench surface	-0.2 to -8.9, to max -46.9	10,00	All except 10 & 00
Bench face	-33.4 to -97.1	18,10,20,99	40,80
Tidal flat	+0.9 to -6.3	18,10,30	80,00
17 July 2013 (260 days of monitoring)			
Floodplain	+1.5 to -12.2	00	All except 00 & 18
Bank crest	-5.1 to -52.8	00,18,00	40, 60-90
Upper banks	-10 to -36.4	18,10,70,90,00,99	30-70
Lower banks	-3 to -37.5	00,50	Variable
Bench surface	-1.4 to -11, to max -60	10,00	All except 10 & 00
Bench face	-40 to -98.4	18,10,20,00,99	40,50,60
Tidal flat	+1.3 to -6.3	18	00,20
28 August 2013 (302 days of monitoring)			
Floodplain	0 to -13	00	All except 00 & 18
Bank crest	-5.5 to -60	00,18,10	40,60,80,90
Upper banks	-10.4 to -50	18,10,00,99	30-80
Lower banks	-2.7 to -44.5	00,50	Variable
Bench surface	-0.3 to -8.8, to max -60	10,00	All except 10 & 00
Bench face	-48.5 to -117.6	18,10,20,30,00,99	40,50
Tidal flat	+7.5 to -6.3	18	20
14 October 2013 (349 days of monitoring)			
Floodplain	0 to -15.2	00	All except 00 & 18
Bank crest	-8 to -67	00,18,10	40,60,80,90
Upper banks	-12 to -70, to max -109.2	00,99	30-80
Lower banks	-5.5 to -64.5	18,00	Variable
Bench surface	-1.4 to -12, to max -80	18,10,00	All except 18,10 & 00
Bench face	-53 to -137.2	18,10,20,00,99	50,60
Tidal flat	+1 to -8.5	18,60-99	10,20
25 November 2013 (392 days of monitoring)			
Floodplain	0 to -17	00	All except 00 & 18
Bank crest	-12 to -69.4	00,18,10	40,60,80,90
Upper banks	-15 to -70, to max -109.2	10,00,99	30-80

GEOMORPHIC UNIT	RANGE OF EROSION MEASURED (CM, CUMULATIVE WITH EACH COLLECTION)	PROFILES WITH THE HIGHEST EROSION	PROFILES WITH THE LOWEST EROSION
Lower banks	-3 to -73	18,00	Variable
Bench surface	-2.1 to -13, to max -88	18,10,80,00	All except 18,10,80,00
Bench face	-53.5 to -146.2	18,10,20,30,90,00,99	50,60
Tidal flat	-2.1 to -8	99	40-60

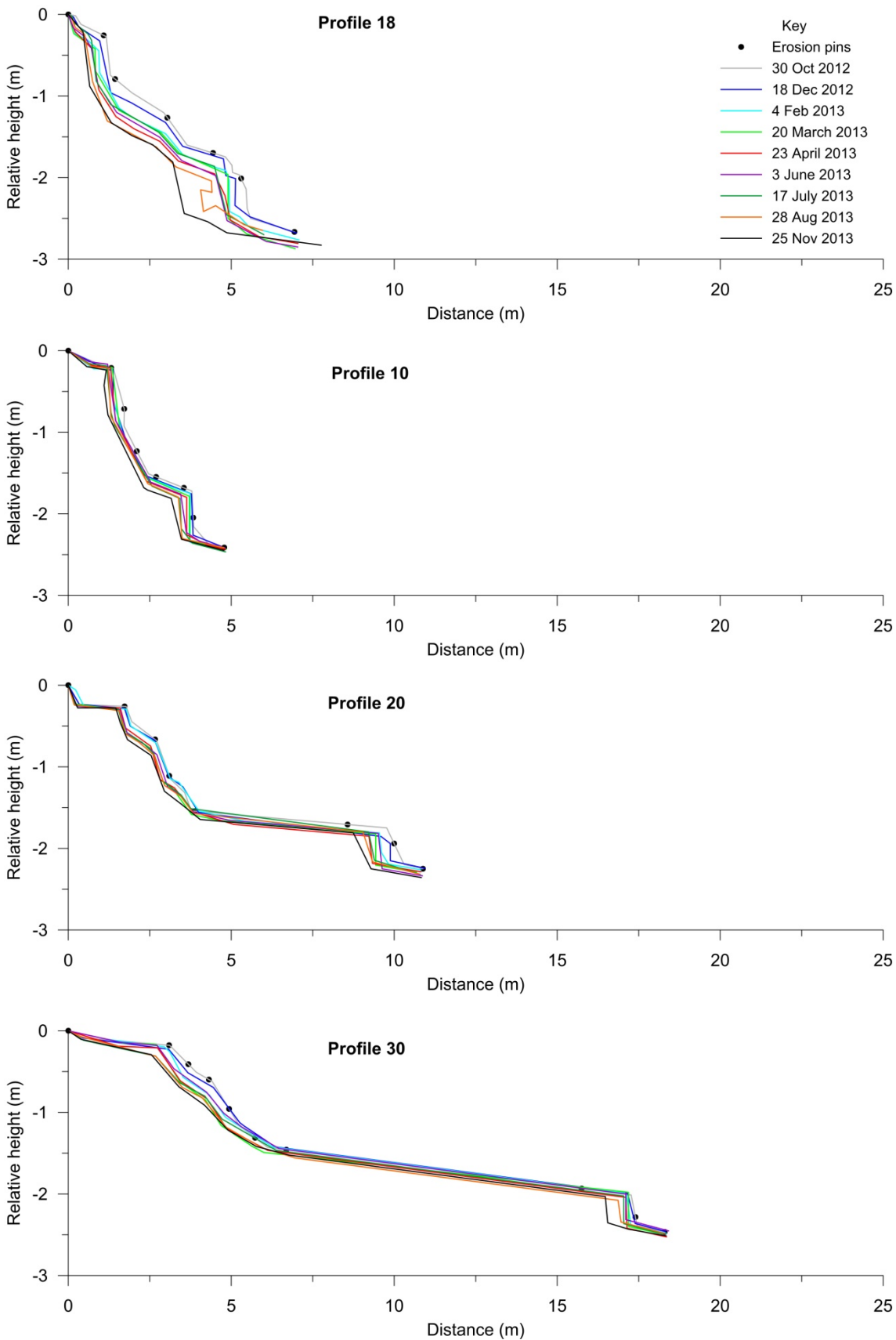


Figure 15. Trends in sediment loss across 8 of the 12 profiles showing parallel retreat of the steeper sub-vertical parts of the banks and minimal downwards erosion of the floodplain and bench surface. Profiles 50, 60, 70 and 90 (not shown) are similar to profiles 50 and 80. The surveys of profiles 18 and 00 show some variability in chronology, particularly on the bench, due to the dislodgement of some pins and re-setting of the transects in as close to their original position as possible. Note the long wave run-up on the bench surface in Profiles 30 to 80.

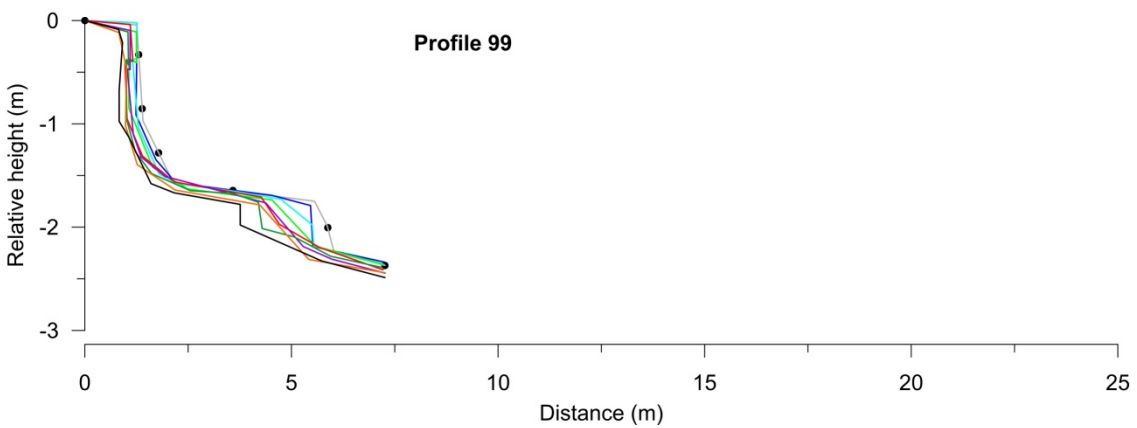
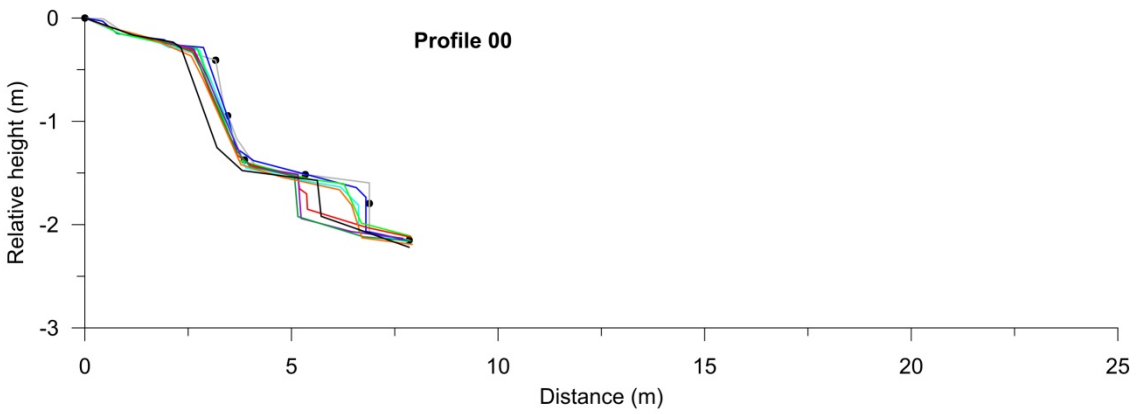
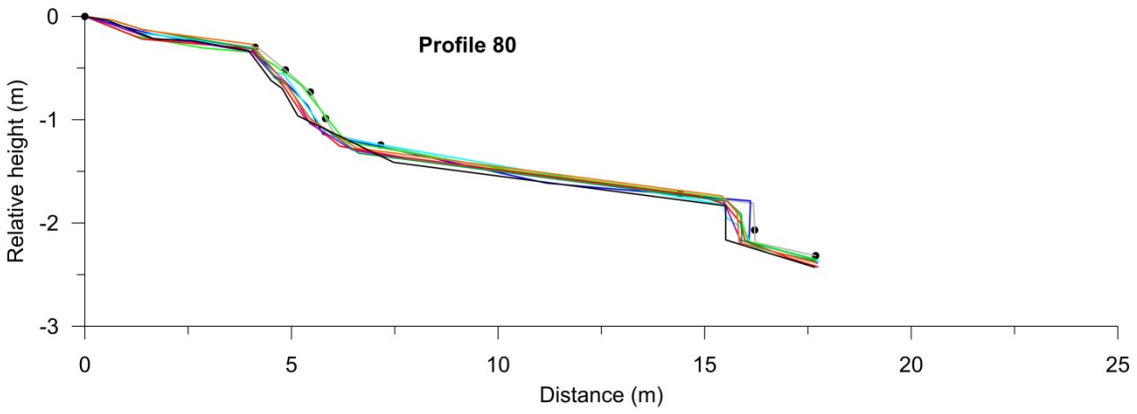
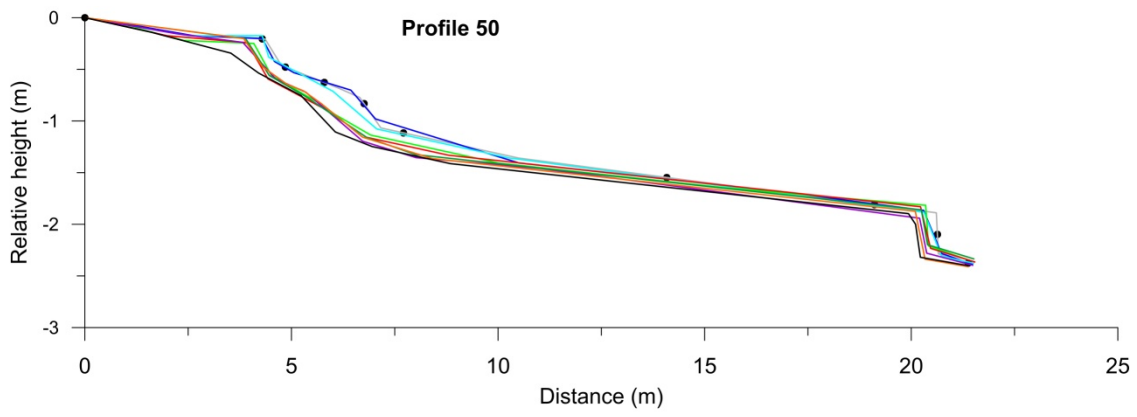


Figure 15. cont.

3.4 Characteristics of storms and tides during the monitoring period

In order to put the erosion rates into context, an analysis of the frequency, magnitude and visual impacts of tides and storms was undertaken to understand the areas of the banks that are most likely to be subject to wave attack during the tidal cycle. The monitoring camera proved extremely useful here since it captured 15-minute images of the site from which the variability in tide heights with respect to the position on the banks was determined (Table 9), as well as the prevailing wave conditions during each high tide (Table 10). Although the images could only be captured during daylight hours, it is reasonable to assume that the relative percentages are similar for high tides that occurred at night as well based on the data from the tide diver and wind speed-direction at the site. The tide diver which recorded tide heights at the site was used to verify the observations from the camera. However, the analysis was based on the camera images since these showed exactly where on the banks that the water level reached during high tide, as well as the characteristics of waves and the interaction of waves on the bank surface.

Of the 479 high tide events that were visually assessed, only 11 % of these did not extend higher than the lower bank-bench boundary. However, up to 16 % of high tides did not reach the bank crest or onto the floodplain. The data shows that the main zone of tidal influence is mostly between the bench and lower-mid banks. The upper parts of the banks including the crest and floodplain were progressively less frequently subject to inundation during the monitoring period.

Around 54 % of these high tides included some wave action whereas 41 % showed calm conditions or ripples indicating that not all high tides were erosive through wave action. Less than 2 % of high tides captured showed medium-large or large waves, but in all cases the water level was always at the bank crest or extended onto the edge of the floodplain. However, high tides that inundated up to the upper banks also occurred under calm conditions including two that were king tides (Table 11). Based on the data, we conclude that the normal tidal range of inundation under calm conditions is from the bench face to the upper banks, and the level of inundation is increased through increasing wave heights.

The camera images at low tide also enabled observations of changes to the banks over the tidal cycle and following large storm events (defined as high tides with medium-large or large waves). These observations included evidence of bank erosion, deposition of sediment particularly sand (and organics), and reworking of sediment including fragments of material eroded from the banks. Note: all of the images showing the conditions at high and low tide are available separately as a time-lapse sequence.

Table 9. Maximum wave position reached during high tides, expressed as a percentage of the total events recorded by the monitoring camera between 1 November 2012 and 25 November 2013.

MAXIMUM WAVE POSITION ON THE BANK AT HIGH TIDE	PERCENTAGE	CUMULATIVE PERCENT
Large area of floodplain submerged	0.4	0.4
At bank crest and onto floodplain	13.4	13.8
Bank crest	2.3	16.1
Upper banks	20	36.1
Mid banks	22.5	58.7
Lower banks	24	82.7
Boundary of lower banks and bench	5.6	88.3
Bench surface	5.4	93.7
Bench face	0.2	93.9
Could not be determined (dirty lens)	6.1	n/a

Table 10. Maximum wave size during high tides, expressed as a percentage of the total events recorded by the monitoring camera. Examples of the wave categorisation used are shown in Fig. 7.

WAVE SIZE AT HIGH TIDE	PERCENTAGE	CUMULATIVE PERCENT
Large waves	0.6	0.6
Medium – large waves	1.3	1.9
Medium waves	11.3	13.2
Small – medium waves	13.2	26.3
Small waves	23	49.3
Ripples to small waves	5	54.3
Ripples	19.4	73.7
Calm	21.1	94.8
Could not be determined (dirty lens)	5.2	n/a

Table 11. Maximum wave position reached during high tides under calm conditions, expressed as a percentage of the total number of events under calm conditions.

MAXIMUM WAVE POSITION ON THE BANK AT HIGH TIDE	PERCENTAGE	CUMULATIVE PERCENT
Large area of floodplain submerged	0	0
At bank crest and onto floodplain	0	0
Bank crest	0	0
Upper banks	12.3	12.3
Mid banks	26	38.4
Lower banks	43.8	82.2
Boundary of lower banks and bench	9.6	91.8
Bench surface	6.8	98.6
Bench face	1.4	100

Between tides, small, gradual changes were evident on a daily basis. These changes included deposition and reworking of sand in three main areas: in front of the bench face, on the bench surface extending to the lower banks, and on the floodplain. The location of sand deposition across the bench surface was not uniform over the monitoring period and instead transitioned from the northern end to the centre and southern end over the year. Eroded bank material was frequently deposited in front of the bench face, but its persistence was limited to a day or a few days indicating removal or rapid break down. Larger fragments (clay balls) deposited on the tidal flats several meters away from the bench face were relatively persistent over several months or longer.

Over short time periods, erosion of the banks was also not obvious. However, over the course of months, horizontal retreat of the bench face was clearly evident, as were erosion of the lower, mid and upper banks, and the position of the bank crest.

Following large storm events, there were obvious changes in the size and location of the sand deposits but these were similar to those observed at other times under the tidal cycle. However, there was no clear evidence of extensive erosion after storm events, only a small section of retreat of the bench face after one event but no obvious signs of erosion of the lower-mid-upper banks across the whole site.

The camera images suggest that the erosion measured during the monitoring period was gradual yet constant over time under the tidal cycle. The larger storm events captured during the monitoring period did not appear to trigger greater erosion relative to the between-storm periods which were characterised by high tides with smaller waves to calm conditions. Hence it appears that even smaller, less erosive waves must be effective at abrading and plucking sediment from the bank surface. We can conclude from the evidence recorded by the camera, that bank erosion at Lang Lang was not solely event driven and instead occurs on a daily basis under the tidal cycle, which over a period of time (months-years-decades) amounts to significant sediment yields into the bay.

3.5 Analysis of wind conditions, fetch and wave energy

The waves in Western Port are wind-generated, hence the importance of wind-wave energy was investigated to identify whether factors like daily or seasonal trends in wind speed and direction, relative to fetch and large-scale bank orientation, play a key role in determining the location, timing and magnitude of erosion at the monitoring site and at other areas where erosion is occurring around the bay.

The observed wind data from the monitoring site, Cerberus and Rhyll show relatively similar, well defined patterns in average and maximum wind speed and direction (Figures 16 and 17). The dominant wind directions at the monitoring site are NNW to WNW (including the strongest winds of $> 70 \text{ km hr}^{-1}$), S to SW and NE to ENE (very light winds). These are consistent with Cerberus and Rhyll which show dominant winds from the N to WNW and S to SW, and a higher proportion of higher speed winds. There is some variability between the sites which probably reflects localised influences such as topography and shielding. The maximum wind gust recorded at the monitoring site was 98.2 km hr^{-1} (on two occasions) and these were from a W and WNW direction.

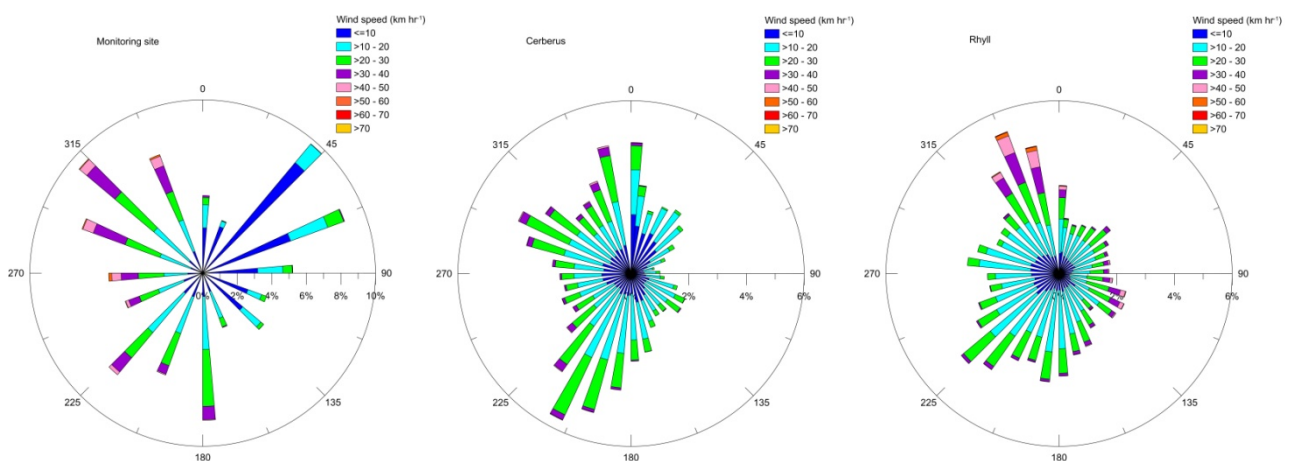


Figure 16. Patterns of average daily wind speed and direction at the monitoring site (~ 13 months data), Cerberus (22 years data) and Rhyll (22 years data). The stacked colours represent increasing wind speeds, while the length of the bars indicates the proportion of winds from each direction.

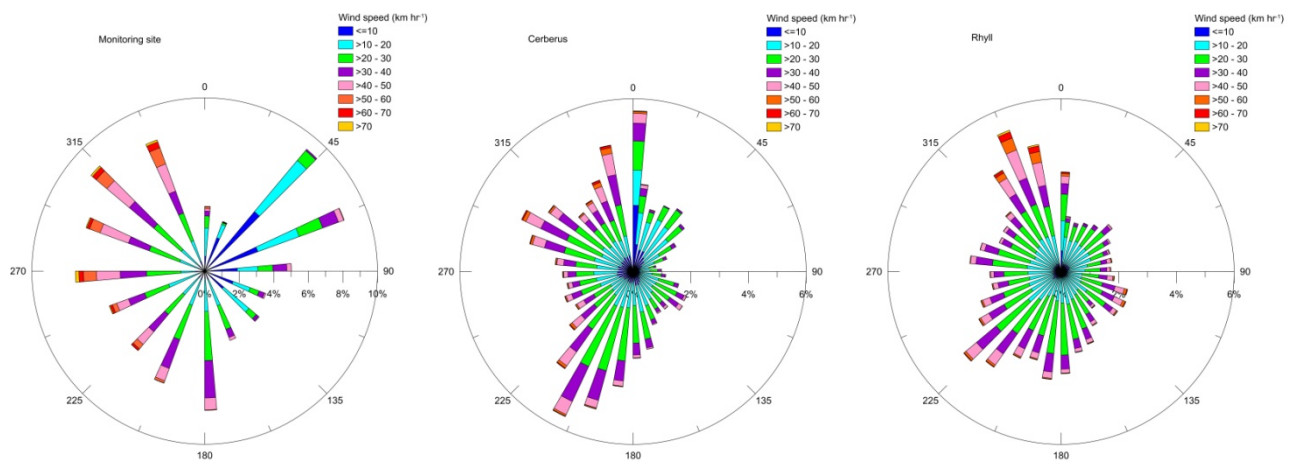


Figure 17. Patterns of highest daily wind speeds at the monitoring site (~ 13 months data), Cerberus (22 years data) and Rhyll (22 years data). The stacked colours represent increasing wind speeds, while the length of the bars indicates the proportion of winds from each direction.

There is very good agreement between the sites in terms of seasonal wind speeds and directions, which reveal strong seasonal trends (Figure 18). In summer, stronger winds are predominantly from S to SW, while in winter these shift to a clear N to WNW direction. In autumn and spring, the dominant wind directions are more variable, with a dominant westwards direction (NNW to SSW). There appears to be very little difference between the autumn and spring patterns, except that the winds in spring appear slightly more westwards and are slightly stronger than in autumn. It is hypothesised that the autumn and spring patterns reflect the transitioning between the strong summer and winter wind directions. At all locations, the highest proportion of strong winds, were recorded in the winter months.

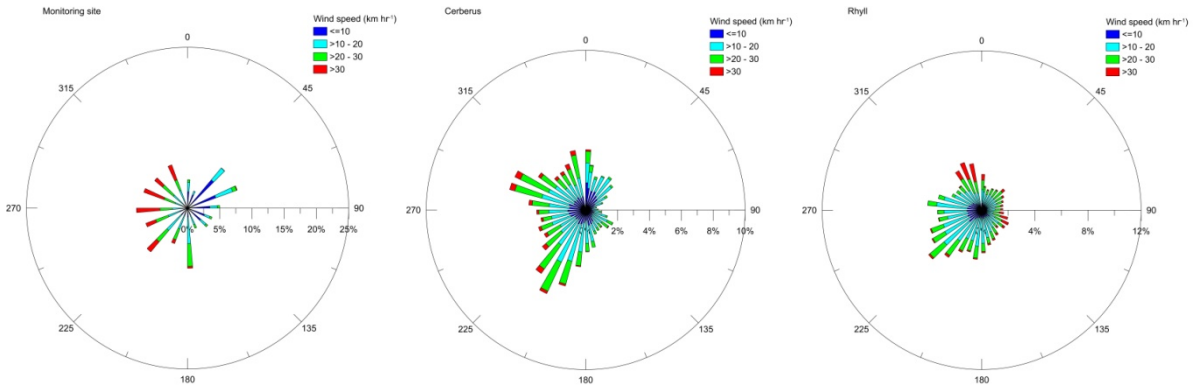
The wind conditions for the days between each erosion pin measurement are shown in Fig 19. These mirror the seasonal patterns shown in Fig 18, with the largest proportion of the strongest winds from the ~NW direction occurring in the winter months (4 June-17 July; 18 July-28 Aug), while the summer months (19 Dec- 4 Feb) show the strong dominance of the S to SW winds. Light winds from the NE seem to be a consistent occurrence throughout the year.

Comparison of the wind data with the erosion pin data reveals some interesting findings. The starting hypothesis would be that the maximum erosion rates are expected to be recorded at the site following the periods of the strongest winds, assuming that wind strength correlates with wave energy conditions and erosion potential, but the data does not show this. Instead, the maximum average erosion rates were measured over the periods, 21 March-23 April (-3.61 cm mth⁻¹) (autumn) and 29 Aug-14 Oct (-3.73 cm mth⁻¹) (spring) when winds were highly variable, with a slight dominance of stronger winds from the ~NW direction. Minimum erosion rates were recorded over the periods from 24 April to 28 Aug (-1.47 to -1.98 cm mth⁻¹) (winter) when there was a dominance of stronger NW winds. Relatively high erosion rates were recorded over summer from 2 Nov to 20 March (-2.61 to -3.12 cm mth⁻¹) when the S-SW winds dominated.

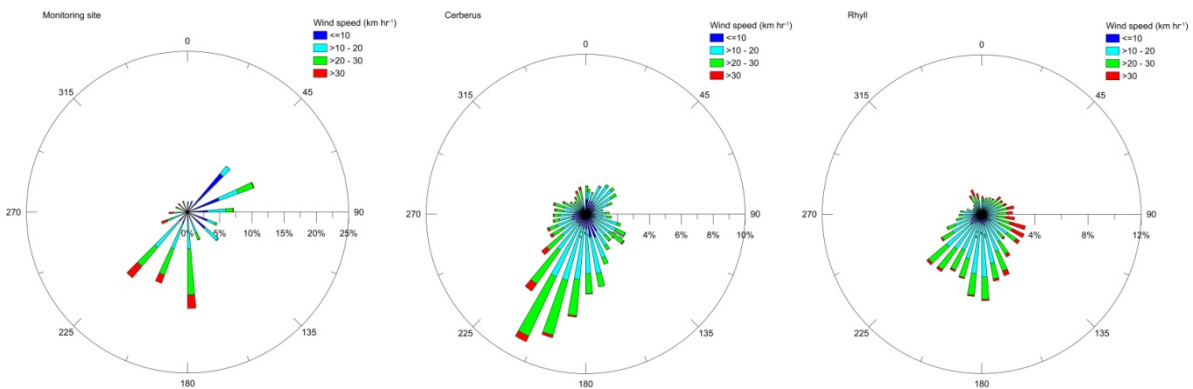
The data suggests that the seasonal patterns of wind speed and direction must not be the only factors influencing bank erosion rates at Lang Lang. The results from the fetch analysis provides an explanation of why. Figure 20 shows the fetch for each wind direction, with the longest fetch indicated in red. A long fetch is important since fetch enhances the height of wind-generated waves, so a longer fetch has a greater impact on wave height than a shorter fetch for the same wind speed.

Because of the influence of French Island, the areas with the longest fetch around the bay vary considerably with wind direction. For example, for a wind direction from the east (90°), the areas with the longest fetch are around Shoreham, Point Leo and north of Hastings, while a for a wind direction from the west (270°) the areas with the longest fetch are the Lang Lang banks and Coronet Bay (for locations, see Fig. 1). Other locations with a significant fetch for given wind directions include Jam Jerrup, Grantville, Balnarring and Somers. It is notable that many of these, particularly those located on the northern and eastern edges of the bay, also experience shoreline erosion (see Fig. 1).

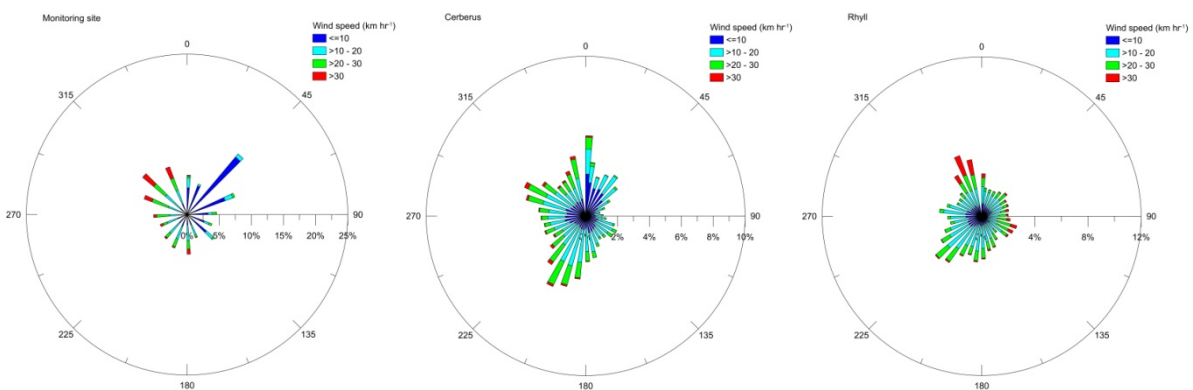
Spring:



Summer:



Autumn:



Winter:

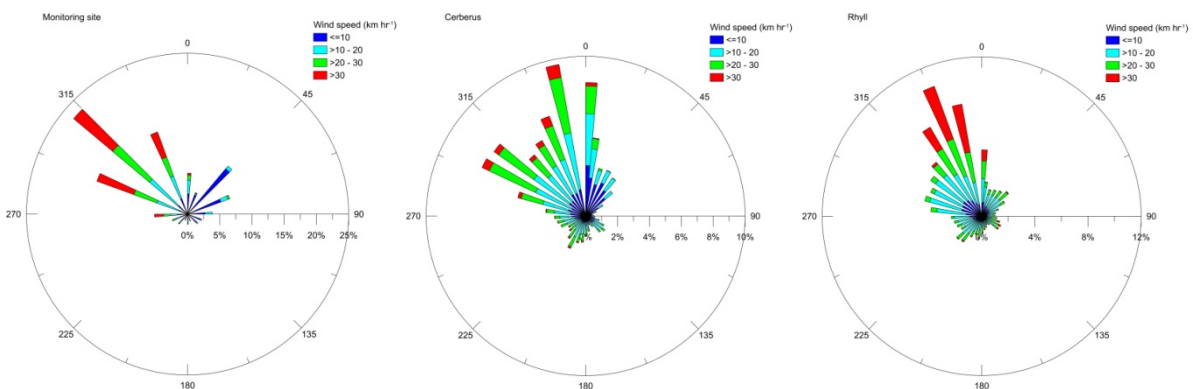


Figure 18. Seasonal trends in daily wind speed and direction at the monitoring site, Cerberus and Rhyll. The stacked colours represent increasing wind speeds, while the length of the bars indicates the proportion of winds from each direction.

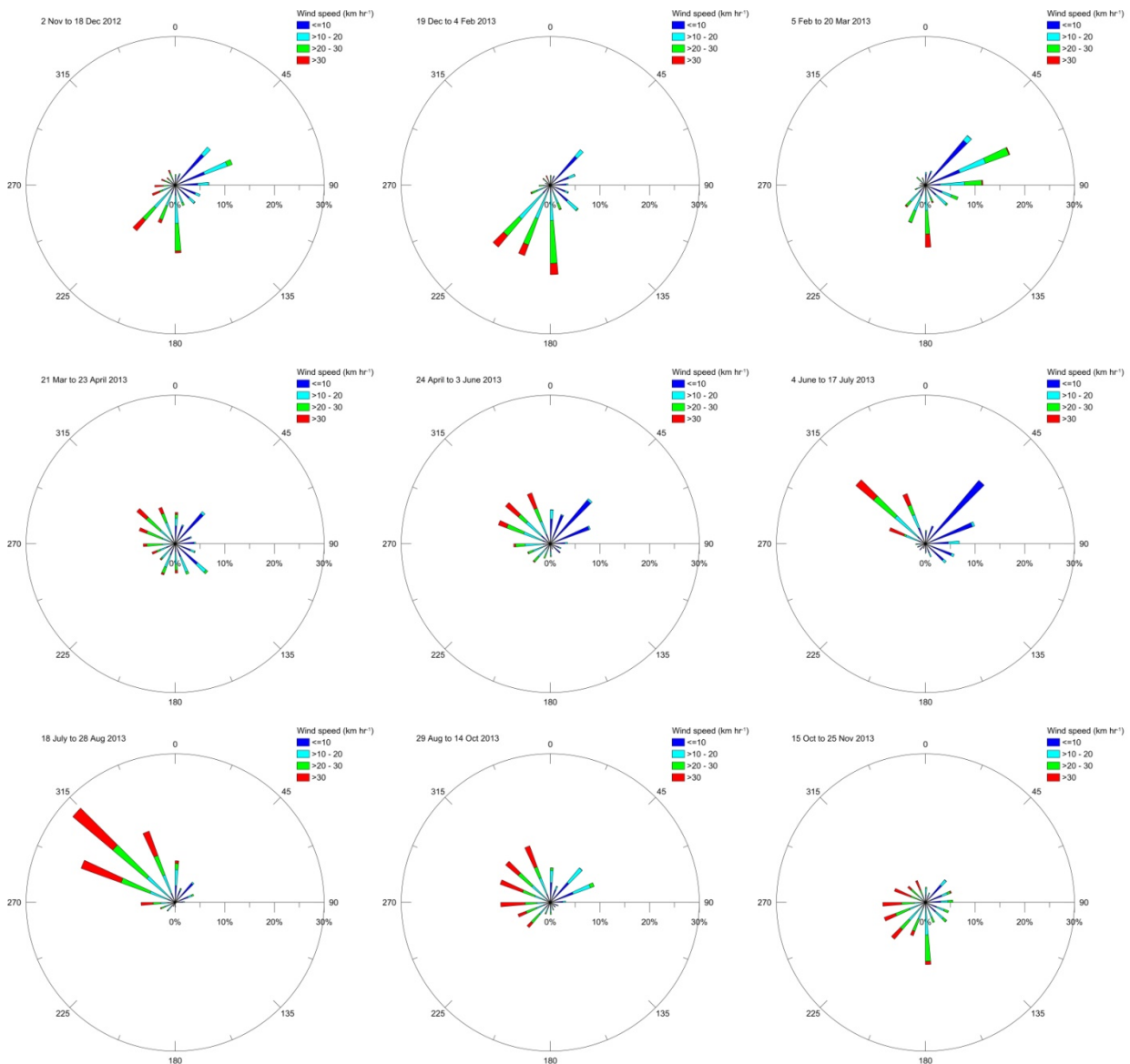


Figure 19. Differences in wind speed and direction at the monitoring site between erosion pin measurements. The stacked colours represent increasing wind speeds, while the length of the bars indicates the proportion of winds from each direction.

For the banks at Lang Lang, the most significant wind direction overall with respect to fetch, is from the west (270°). For the northern and southern ends of the banks, wind directions of WSW (247°) and WNW (292°), respectively, are also significant. Other wind directions with a relatively long fetch are SSE (157°), SW (225°) and NW (315°). The wind directions with the shortest fetch and hence, the least (or nil) impact at the site are from the NNE to ESE ($22^\circ - 112^\circ$).

At the monitoring site, a summary of the seasonal patterns of wind direction, compared to fetch (Fig 21), highlights the importance of these factors on wind-wave potential and likely erosion rates. Winds from the W and WSW in autumn and spring have the longest fetch (17.7 km and 13.3 km, respectively), followed by winds from the WNW in winter, autumn and spring (10.4 km) and southerly winds in summer, autumn and spring (9.7 km). Comparison with the erosion pin data shows that the monitoring period that recorded the highest erosion rates (29 Aug – 14 Oct) also recorded the largest proportion of the strongest westerly winds thus supporting the role of fetch as a major factor. The relatively high summer erosion rates, compared to the lower erosion rates recorded in winter, also in part can be explained by fetch and the prevailing wind conditions recorded at the site over the ~13 months. However, the patterns are not entirely clear for all of

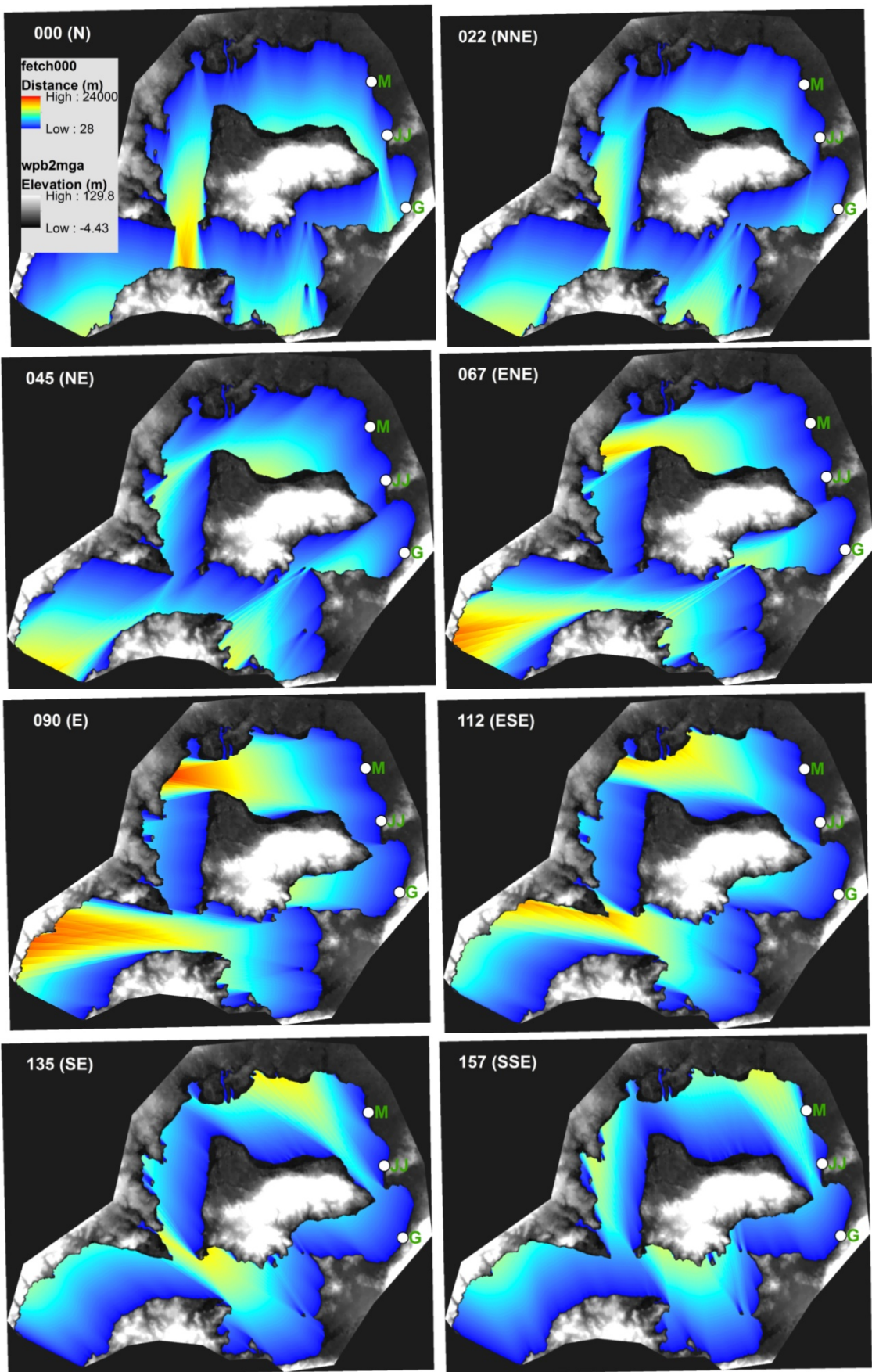


Figure 20. Patterns of fetch for each wind direction. The scale for all plots is shown in the plot labelled 000, while M is Monitoring site, JJ is Jam Jerrup and G is Grantville. The areas of the bay that have the longest fetch are indicated by red-orange, while dark blue indicates the shortest fetch. Note how these patterns change with wind direction.

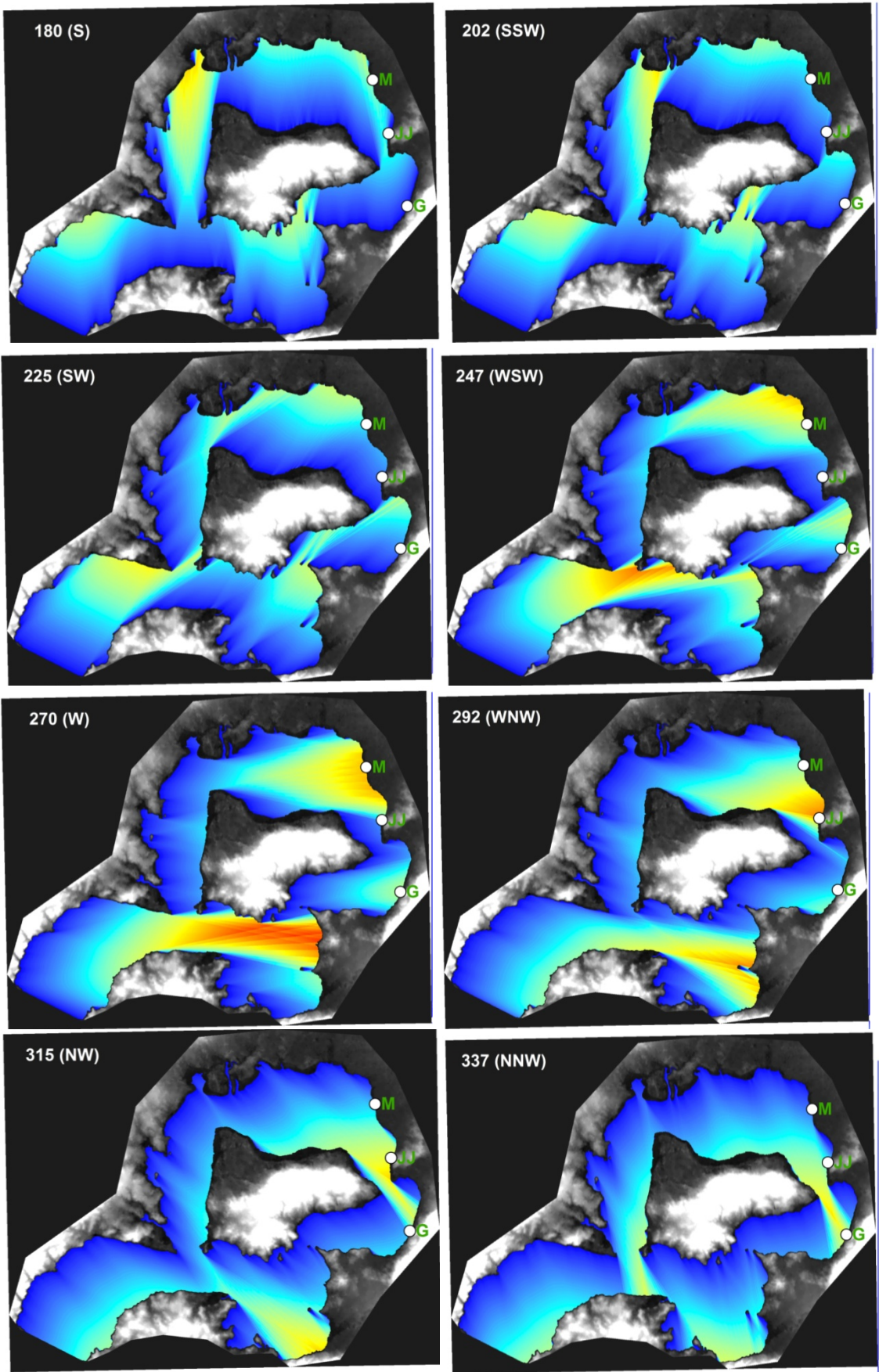


Figure 20 cont.

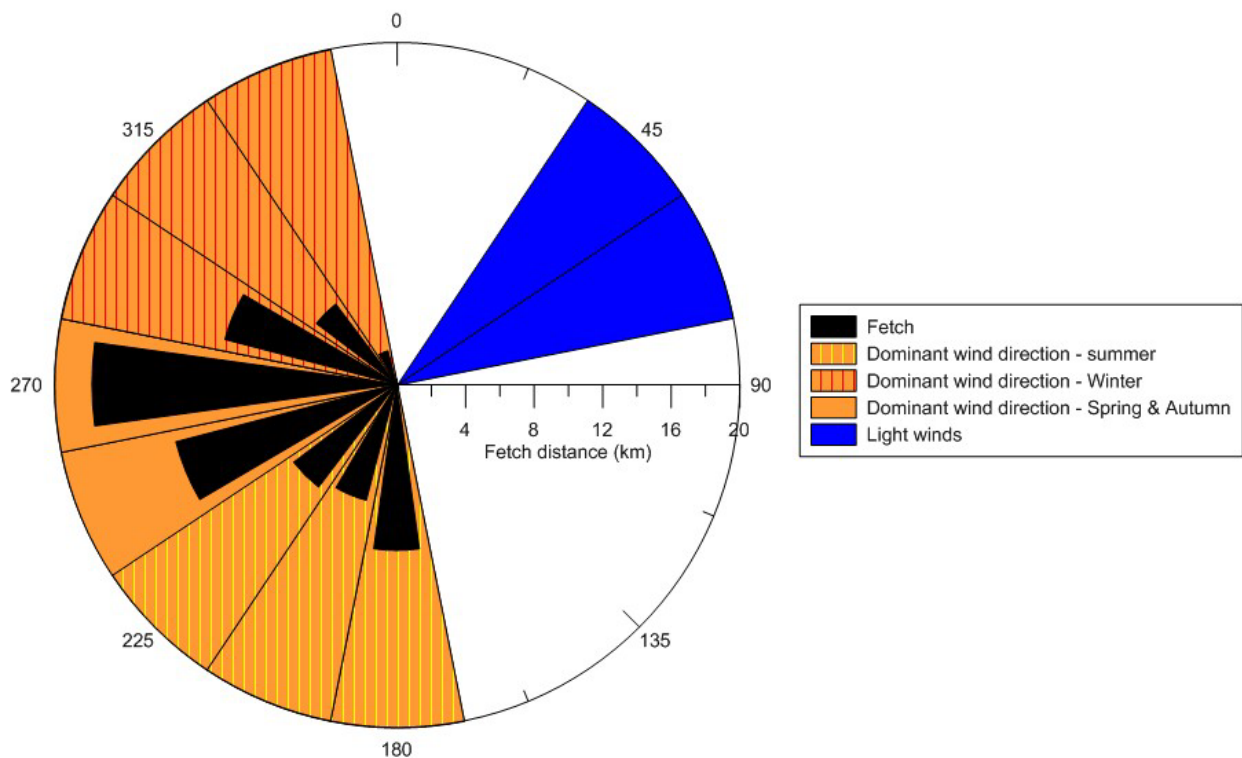


Figure 21. Summary of the seasonal wind patterns and fetch for each direction at the monitoring site. The data shows that winds from the W and WSW in autumn and spring have the longest fetch, followed by winds from the WNW in winter (& spring and autumn) and southerly winds in summer (& spring and autumn). Winds from these directions have the potential to generate greater wave heights compared to winds of similar speeds from different directions. The light winds from the ~ NE that were recorded throughout the year, have ~ zero fetch and hence no impact on erosion at the monitoring site.

the erosion rate measurements. Other factors such as variability in tide heights affecting the height of inundation of the banks (e.g. Table 9) have probably also been an important control on the erosion data.

To further explore this, simple wave modelling was undertaken to investigate the impacts of fetch, wind speed-direction and tides on wave height and wave power at three sites with significant erosion around the bay. For the monitoring site, the calculated wave power was also compared to the erosion pin data to identify any correlations.

The results showed that wind speed and fetch direction have a significant impact on wave power at the three sites. For a water depth of 2 m (i.e. the highest of the high tides), the calculated values range from <0.01 to a maximum of 28 kW m⁻¹ in response to 100 km hr⁻¹ winds (Fig. 22). While the wind direction with the highest wave power at the monitoring site is west (26.4 kW m⁻¹), at Jam Jerrup the highest wave power occurs in response to 100 km hr⁻¹ winds from the WNW and NW (27.6 kW m⁻¹ and 21.9 kW m⁻¹). At Grantville the highest wave power occurs in response to strong winds from the W (17.5 kW m⁻¹) and NNW (17 kW m⁻¹). Winds from the NE to SSE have a very low (<0.01 kW m⁻¹) to zero wave power at all three sites regardless of wind speed.

Using the average 30-minute wind speed-direction data, along with the tide data to indicate water depth and modelled wave height, wave power was then calculated for the three sites to derive the 30-minute average wave power conditions during the monitoring period. These were also summed to derive daily totals (Fig. 23) noting that during low tides and under calm wind conditions wave power is zero. On a daily basis, the data shows differences between the sites in terms of total wave power, reflecting those differences that were identified in Fig. 22. For the monitoring site, the maximum 30-minute wave power was 7.08 kW m⁻¹ (28 September 2013, 10 am) while the maximum daily total wave power was 75.8 kW m⁻¹ (17 October 2013). At Jam Jerrup, the maximum 30-minute maximum was slightly higher at 7.45 kW m⁻¹ (28 September 2013 9:30 am) and maximum daily total was also slightly higher at 86.7 kW m⁻¹ (5 July 2013). At Grantville, the maximum 30-minute and daily total wave power were 5.6 kW m⁻¹ and 59.6 kW m⁻¹ respectively; both of these occurred on 18 August 2013.

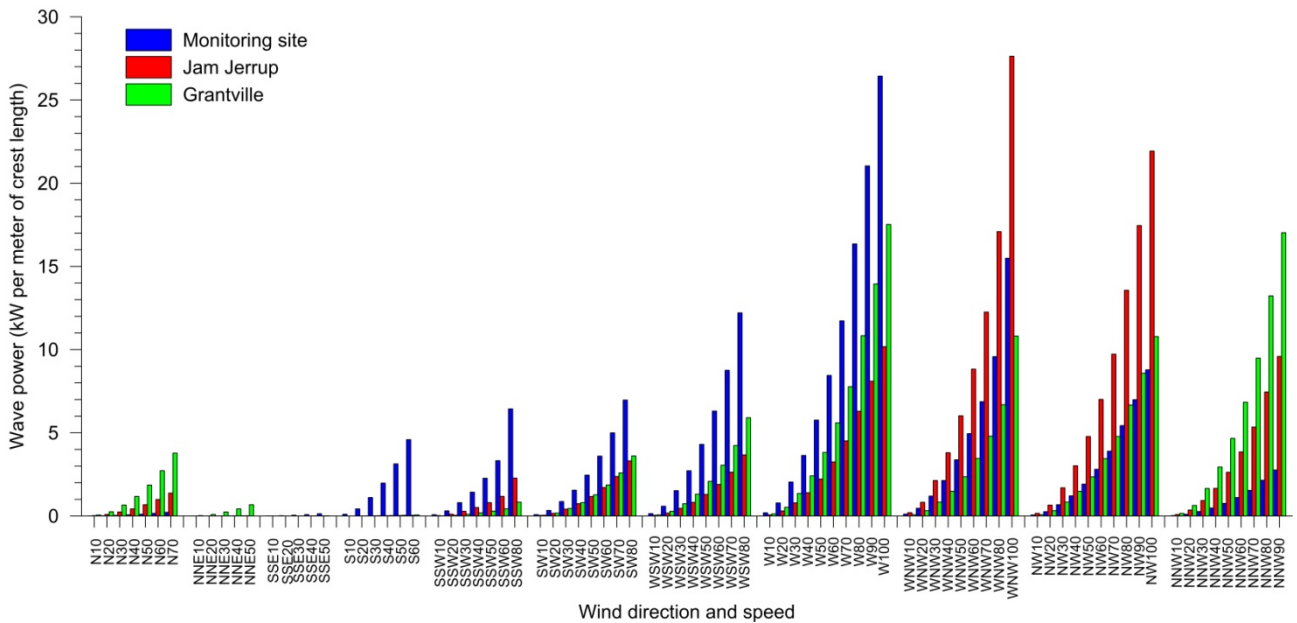


Figure 22. Maximum wave power predictions for different wind speeds ($10\text{--}100\text{ km h}^{-1}$) and directions at the monitoring site, Jam Jerrup and Grantville, assuming a water depth of 2 m which is equivalent to the maximum high tide recorded. The wave power predictions for winds from the NE, ENE, E, ESE and SE are not shown since these values are $< 0.1\text{ kW m}^{-1}$ for all wind speeds.

One of the critical questions in this study is: does wave power explain (and control) the trends in measured sediment loss over the monitoring period? Figure 23 shows the sediment loss calculated from the erosion pins, plotted against total daily wave power. While there is some evidence to suggest that a higher wave power correlates with a larger sediment loss (Fig. 24), especially over the August-September-October months, the relationship is weak. The results are also not consistent over the entire monitoring period. The calculated wave power for the January-May period is much less than the July-November period, despite equal or higher average sediment losses from the banks (Fig. 23).

There are four possible explanations for this. First, the Lang Lang coastline is strongly crenulated and there is a high degree of variability in the orientation of the banks over short distances ($< 100\text{ m}$) meaning that different parts of the headlands and crenulations will be more/less exposed to different wind directions. The monitoring site is a good example, where profiles 10, 20, 30 and 40 are largely protected from the direct impact of S to SW waves, but are directly exposed to waves from the NW. Whereas, for profile 90 the opposite is true, while profiles 18, 00 and 99 on the headlands are exposed to all waves from a general westerly direction. The resolution of the wave modelling, which is based on the resolution of the DEMs (28 m pixels) was too coarse to capture this small-scale variability in the orientation of the coastline. Further work to investigate the impacts of bank orientation could include higher resolution wave modelling.

The second explanation is that it is assumed here that waves travelling perpendicular to the banks will cause the greatest erosion through direct absorption of wave energy on the bank surface. However, it was also observed at the monitoring site that waves travelling parallel to the banks, either as a result of the dominant wind-wave direction or because of wave refraction around the headlands, performed a ‘sweeping’ motion. In places, this sweeping motion resulted in minor undercutting or was seen to enhance erosion along cracks in the bank surface. The relative contributions of erosion by direct absorption of energy versus parallel ‘sweeping’ could not be determined in this study. However, the subject could be the focus of further work by measuring the localised variability in the energy distribution of waves around the crenulations.

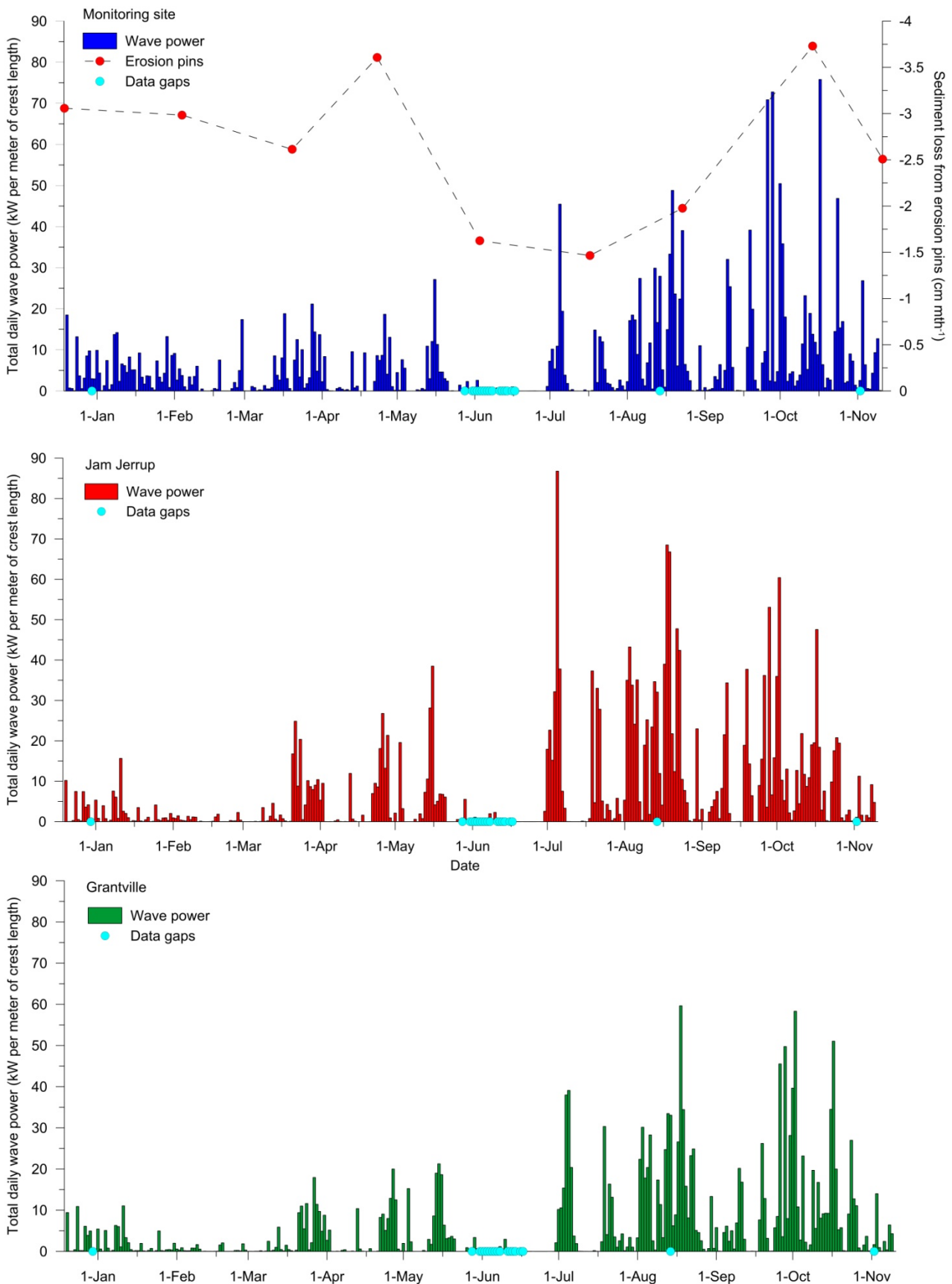


Figure 23. Total daily wave power at the monitoring site, Jam Jerrup and Grantville. Wave power was calculated using the wind speed-direction and tide data, and modelled fetch and wave heights. Data gaps shown in the plots are due to gaps in the wind speed-direction data. These were due to occasional problems with the weather station.

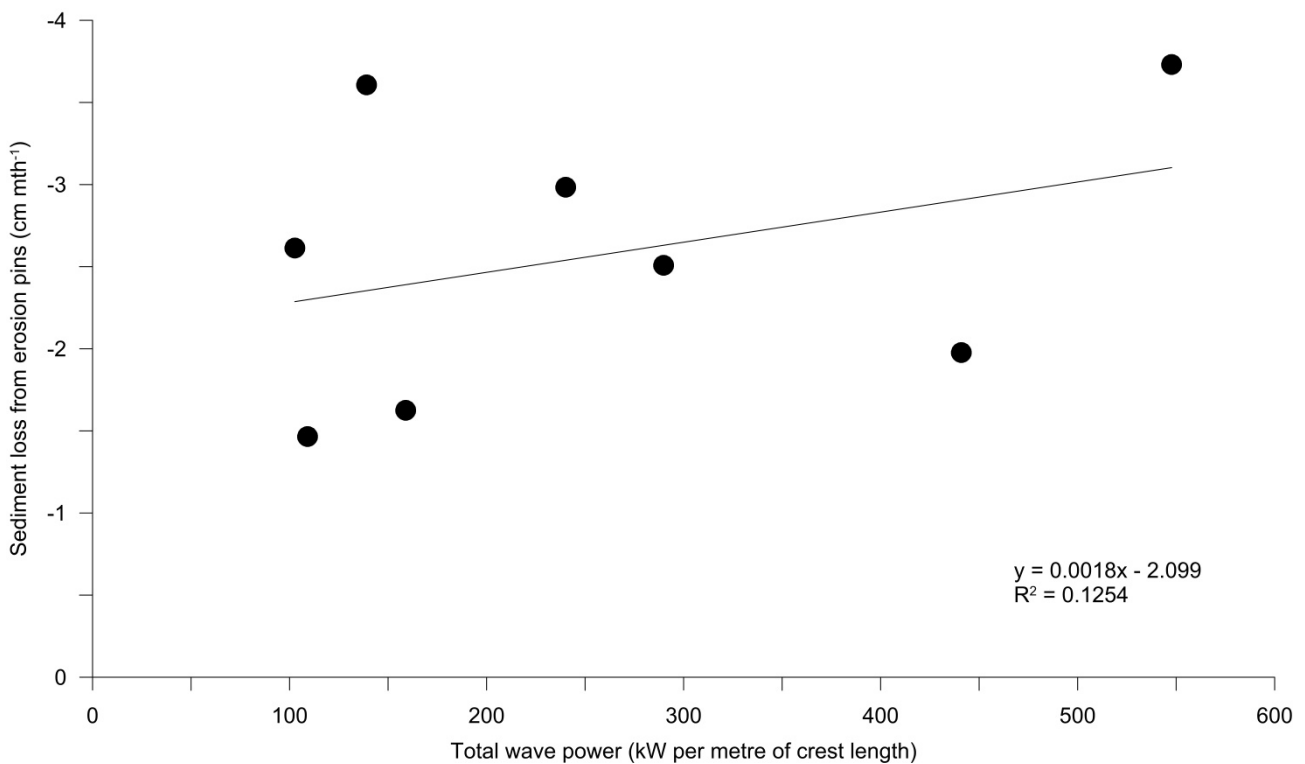


Figure 24. Sediment loss versus wave power at the monitoring site, summed to represent totals for the erosion pin measurement periods. The data show a weak positive relationship between sediment loss and wave power.

The third explanation is that there may be a threshold of wave power, above which erosion occurs regardless of the size of the waves. That is, erosion occurs through the presence of wave action, and the amount may be irrespective of the power of those waves above a certain threshold. The camera images showed that more than 50 % of high tides had some wave action and that there was no obvious visible (or catastrophic) erosion at the monitoring site following large storm events, only movement of sand deposits. Both observations lend support to this explanation. Therefore it is concluded that daily wind-wave erosion during high tides is an important component of the total sediment yield into the bay. Further work could include more sophisticated hydrodynamic modelling to evaluate the theory and establish if such thresholds exist.

The fourth explanation relates to the repeated wetting and drying of the surface sediments, which leads to cracking that can enhance the effectiveness of physical erosion processes such as plucking and abrasion during wave attack. The monthly trends in evaporation from the nearby Bureau of Meteorology station, CSIRO Aspendale (period of record 1965-1982) (Fig. 25 and Fig. 26) show a very good correlation with the trends in the erosion pin data, implying that drying and cracking of the banks through evaporation, in between wetting associated with the tidal cycle, must be an important control on erosion (along with the shrink-swell properties of the clays and high salt concentration of the bay water). The evaporation data shows that in the summer months, evaporation is 1 to 2-times greater than in the winter months (Fig. 25). While we did not explicitly measure evaporation and the degree of shrink-swell, we did observe over the course of the monitoring period under similar weather conditions (i.e. fine and sunny) that there was much greater drying and cracking of the surface of the banks in summer during low tide (see Fig. 8 as an example), compared to the bank surface in winter during low tide.

It is highly probable that enhanced wetting-drying and cracking of the bank surface facilitated the higher erosion rates measured on the 18 Dec (2012), 4 Feb, 20 March and 25 Nov (2013), whereas in June-July, the bank surface remained relatively moist and smooth accounting for lower erosion. The 14 Oct erosion rate can be explained by a combination of wave power and evaporation. However, the explanation for the relatively high 23 April measurement is still unclear. Further work to test the importance of wetting and drying on erosion could involve experimental work on sediment behaviour under different seasonal climate conditions.

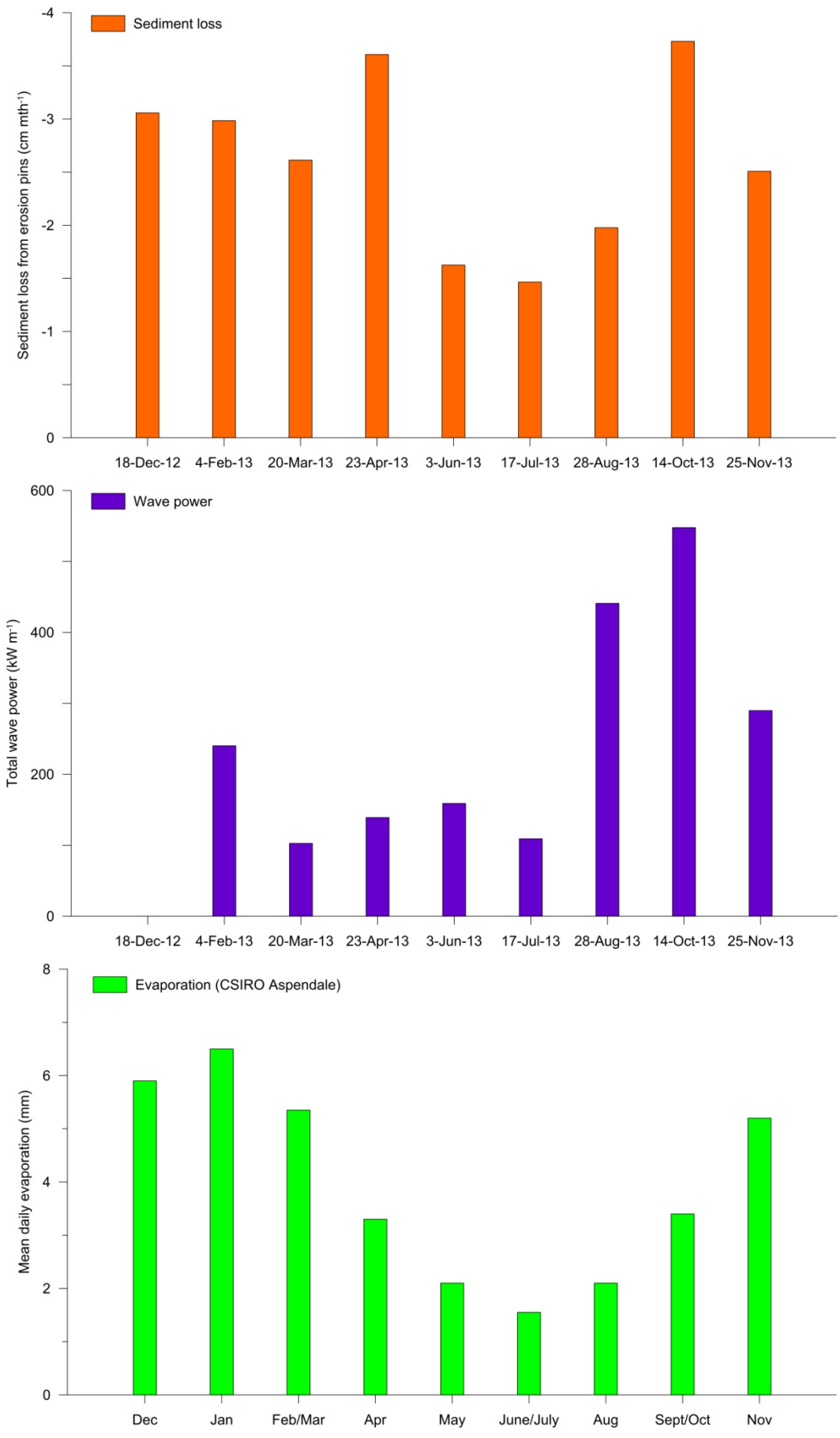


Figure 25. Sediment loss and total wave power for each erosion pin measurement period at the monitoring site, compared to monthly trends in evaporation recorded at the nearby CSIRO Aspendale station.

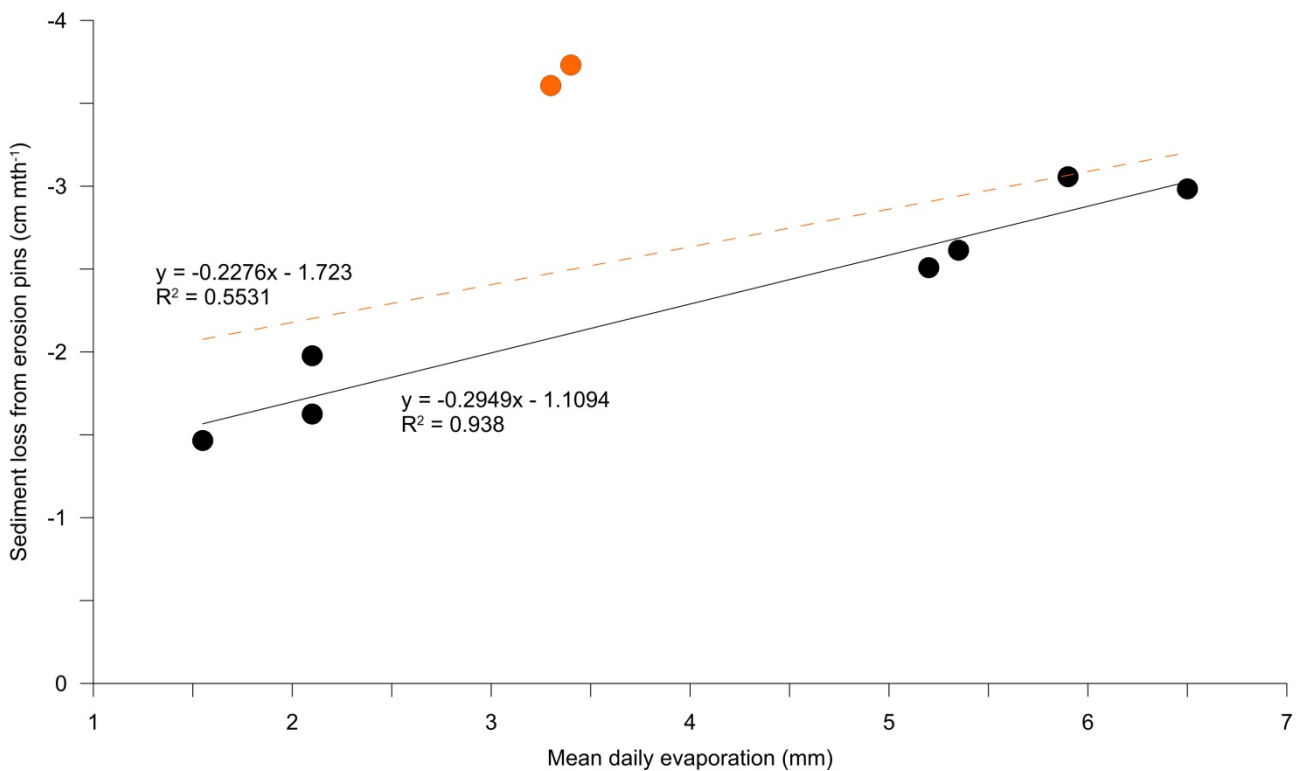


Figure 26. Sediment loss versus evaporation recorded at the nearby CSIRO Aspendale station. The orange line indicates the trend through all the data. The black line indicates the trend through the data coloured black, excluding the two orange points which represent the 23 April and 14 October erosion pin measurements. With the exception of the April and October measurements, there is a very good correlation between sediment loss and evaporation, with evaporation affecting the degree of cracking of the surface through shrink-swell of the clays. For the April and October measurements, in addition to evaporation, other factors such as wave power appear to influence erosion rate.

3.6 Examination of trends in groundwater levels in the banks

The final part of the analysis in this study was to establish whether there was any groundwater influence on bank failure at Lang Lang. The observations at the site had already revealed that there was no evidence for bank failure by slumping, which is the mechanism by which failure would occur if there was a rapid change in pore water pressure associated with the rise and fall of water in the bay under the tidal cycle. There was also no evidence at the monitoring site for rapid discharge of groundwater from the banks, only minor seepage in places. However, to support the observations, the groundwater heights and EC data were also collected to prove or dis-prove the impact of groundwater on bank erosion.

Figure 27 shows the groundwater, tide and rainfall results. There is no evidence of rapid groundwater recharge or discharge in response to the tidal cycle, despite the piezometer being located within 10 m of the edge of the banks and the data showing that several times the groundwater levels were below the maximum height of the high tides thus creating a hydrological gradient into the banks. Instead the data shows that groundwater recharge correlates directly with rainfall events, and that these events were followed by a slow period of discharge until the next rainfall (recharge) event. This is consistent with the observations of minor seepage from the banks. The EC data were also lower in the piezometer than the bay, indicating an increased component of freshwater from rainfall.

On the basis of the groundwater results and the consistency in the sedimentology of the banks over 8.6 km, we conclude that pore water pressure is not a causal factor of bank erosion at Lang Lang. We would expect that similar findings would apply to other sites around the bay with a similar sedimentology. However, where sites have a different sedimentology, pore water pressure created by rapid fluctuations in groundwater and tide heights may still be an important factor in bank erosion.

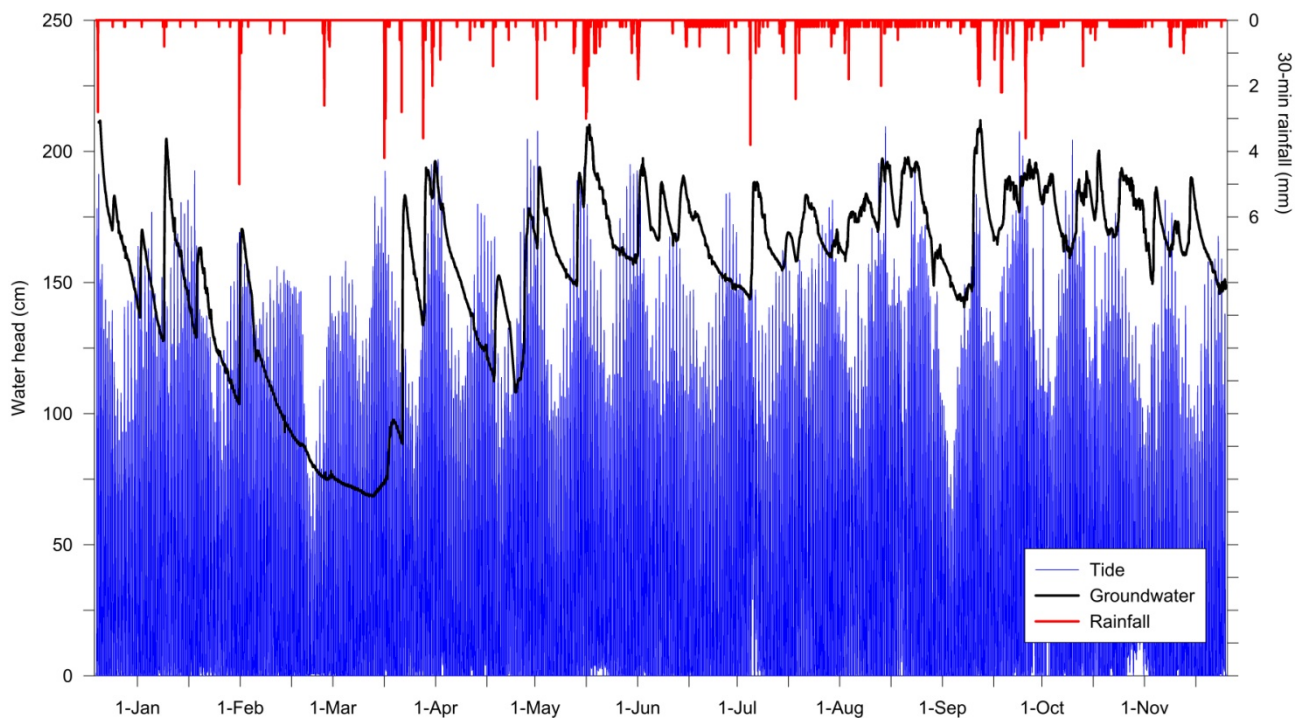


Figure 27. Groundwater levels, tide heights and rainfall at the monitoring site. Note, the groundwater data were corrected for AHD so that they are directly comparable with the tide data.

4 Summary and management implications

4.1 Summary of new knowledge of sediment inputs from bank erosion

This study is the first to provide quantitative data on the contemporary coastal clay bank erosion rates and sediment inputs into Western Port. The study addressed several key research questions relating to the long- and short-term rates of erosion from an 8.6 km stretch of coastline, focusing on a representative monitoring site in detail. The study also examined the major spatial and temporal controls on bank erosion. Based on the results and analysis we draw the following conclusions:

- *Average rates of erosion and sediment inputs:* The rates of horizontal bank erosion at Lang Lang over the study period were on average 0.31 m yr^{-1} , which equates to an average sediment yield of 6.2 kt yr^{-1} , compared to a long-term average of $4.2 \pm 2.9 \text{ kt yr}^{-1}$. Over the timeframe of decades, the likely range is of the order of 0.3 to 1 m yr^{-1} (horizontal bank retreat) and 3 to 10 kt yr^{-1} (sediment yield), although it is possible that erosion rates and sediment yields could equal or exceed 1 m yr^{-1} and 10 kt yr^{-1} , respectively, in a single year. We estimate that the area of land lost through bank erosion at Lang Lang over the last 65 years has been around $233,000 \text{ m}^2$ which equates to a total sediment input into the bay of 270,000 tonnes since 1947. These results are reasonably consistent with previous estimates by Wallbrink *et al.* (2003) and Hurst (2012), when those estimates are adjusted to account for differences in assumptions of bank height, length and sediment bulk density. Thus, our results are consistent with approximately 30% of fine sediment delivered to the bay being derived from coastal bank erosion, as previously estimated (Wallbrink *et al.*, 2003).
- *Composition of sediment inputs:* The composition of the bank sediment at Lang Lang is mostly fines, comprising $\sim 60\%$ clay and $\sim 20\%$ silt. There is also a proportion of very fine to fine sand, $\sim 20\%$, and a minor proportion of organics ($< 10\%$). The erosional susceptibility of the bank material is low due to the high clay content and low dispersibility of the sediment. However, the erosion potential of the surface overall and the bench unit in particular, is enhanced by several factors: surface wetting and drying, shrink-swell of the clays leading to surface cracking, and bioturbation (these are outlined further below).
- *Dominant erosion processes:* Erosion occurs entirely through physical erosion processes during high tides, namely abrasion and plucking of sediment from the bank surface by wave action, and very occasionally minor undercutting and collapse of the banks. The wearing away of the banks by wave energy is in part retarded by the strong resistance of the sedimentary layers. This is reflected in the bank morphology, particularly the formation of a prominent bench. Most of the erosion is occurring on the vertical to near-vertical surfaces leading to parallel retreat of the banks. There is very little downward erosion of the horizontal surfaces such as the bench surface. Passive erosion processes such as bank slumping, which are characteristic of rapid fluctuations in pore water pressure within the banks, are not active at this site.
- *Overall trends set within the context of spatial and temporal variability:* There is considerable spatial variability in erosion rates and hence sediment yields, which ranges from the scale of geomorphic units, to much larger scales (i.e. the length of the Lang Lang coastline). There is also considerable temporal variability in erosion that occurs on sub-daily (tidal), daily, seasonal, annual and decadal timescales. In general, erosion is occurring on a daily basis driven by the semi-diurnal tidal cycle, rather than being event-driven. This results in a continuous daily input of sediment into the bay, with the amount varying spatially and temporally according to the relevant controls (outlined below). There appears to be a long-term trend for the overall smoothing of the Lang Lang coastline. The air photo evidence shows that the crenulations are becoming less pronounced since at least 1947. This is consistent with the monitoring data where faster erosion rates were measured on the headlands (up to 66 cm over the monitoring period) compared to the apex of the crenulation at the monitoring site.

- *Major spatial controls on erosion:* There are two primary spatial controls on erosion -
 - Sediment characteristics: This influences the erosional susceptibility and potential erosion rates. The alluvial sedimentary units at Lang Lang are laterally continuous over the 8.6 km, meaning that there is a similar likelihood of erosion over this distance. We also expect that the potential erosion rates along the total length of the Lang Lang coastline are similar to those measured at the monitoring site. Shrink-swell of the clays combined with alternating wetting and drying of the bank surface over the tidal cycle, is leading to cracking of the surface sediments during low tide. This enhances the effectiveness of the physical erosion processes (mechanical detachment) and hence erosion rates. Another factor that increases the potential for erosion is the formation of bioturbation holes (primarily crabs) and the decomposition of organics contained within the sediments (primarily relict tree roots and stumps). These increase the erodible surface area and enable fragments of material to be more easily dislodged.
 - Orientation of the coastline relative to the dominant wind-wave direction(s) and the direction(s) of longest fetch: This influences wave power and the likelihood of erosion since wave energy is a key driver of physical coastal erosion processes (noting that further work on wave power and erosion rates is required, which is outlined below). There are well defined wind patterns across bay and these are dominated by strong winds from all westerly directions, particularly the SW and NW. We propose that, along with the alluvial sedimentology, the orientation of the Lang Lang coastline is the primary explanation for why this site is eroding. The coastline has a long westerly exposure, and at the monitoring site, the most significant wind-wave directions in terms of the longest fetch and highest potential wave power are (in order of importance): W, WSW, WNW, S, SW and NW. Wave power is predicted to reach a maximum of 26 kW m^{-1} here in response to 100 km hr^{-1} winds from the west.
- *Major temporal controls on erosion:* There are three primary temporal controls on erosion –
 - Semi-diurnal tidal cycle: The extent and timing of erosion is governed by the frequency-duration of high tides (which occur twice per day) and the conditions during each high tide. These conditions include i) the maximum height of each high tide (including daily tidal asymmetry), which determines the extent of inundation and the area of the banks that are subject to wave attack; and, ii) the presence of wind-generated waves, which determines wave power and erosivity. More than 50 % of the high tides observed at the monitoring site showed wave action on the banks and hence erosive conditions. Whereas for a substantial proportion of high tides, calm (non-erosive) conditions prevailed. The main range of tidal influence on the banks is from the bench to the lower-mid banks. It was only during very high tides, and storm events (which occurred < 2 % of time over the monitoring period) that the extent of inundation was much greater. On some occasions the water level in the bay was enhanced sufficiently by large waves to breach the edge of the banks and inundate parts of the floodplain facilitating erosion of the uppermost sedimentary layers.
 - Seasonal wind patterns: The waves in Western Port are wind-generated waves, hence the presence of wave action on the banks and the size and direction of those waves is governed by the prevailing wind patterns (and fetch). There are strong seasonal patterns in wind speed and direction at the monitoring site and across the bay. The dominant wind directions in winter are from the NNW to WNW, while in summer the dominant winds are from the S to SW. In autumn and spring, the winds are more variable but include an overall westwards component. While the summer and winter wind patterns are a significant temporal control on erosion at the monitoring site, it is during autumn and spring that strongest winds from the west are most likely to occur.
 - Seasonal evaporation: There are strong seasonal trends in evaporation which influences the extent of drying of the bank surface, and in turn, the degree of surface cracking during each low tide. The wetting-drying effects of the bank surface appears to be more pronounced in the summer months through significantly higher evaporation compared to winter (1-2-fold increase) (noting that further work on sediment behaviour under different seasonal climate conditions is required, which is outlined below). Enhanced cracking of the surface increases the effectiveness of the physical erosion processes and wave attack during high tides.

4.2 Further work

In addition to the new knowledge gained on the rates and controls on bank erosion, this study has also highlighted some areas that would benefit from further work. In particular, there is a need to address the spatial and temporal controls on erosion in greater detail, and to test the four explanations put forward to explain the patterns of erosion measured at the monitoring site (i.e. bank orientation at the scale of the crenulations, the importance of wave direction on erosion, establishment of wave power thresholds and the role of seasonal evaporation in influencing the extent of drying, cracking and erosion of the surface).

We were unable to monitor the impacts of shoreline orientation at the scale of the crenulations. However, the analysis of bank morphology (i.e. the trends in vertical, sloping and benched banks), the observations from the air photos (i.e. the trend for greater erosion on the north-west facing sides of the crenulations, compared to lesser erosion on the south-west facing sides) and the results from the wave modelling points to small-scale bank orientation as a potentially important factor that may have a large influence on erosion rates. Further work could include higher resolution wave modelling and potentially higher resolution data collection including energy probes. This work could also measure wave power for different wave directions and establish if wave power thresholds exist.

We also established that there are strong seasonal wind patterns across the bay and that these wind patterns in conjunction with fetch and tide heights, have a major impact on wave height and wave energy at the coastline. Further work could involve an analysis of the historical wind records to investigate whether there have been changes in the long-term wind-wave patterns that may explain the decadal-scale variability in erosion rates determined from the air photos. The analysis could also be set in the context of climate change modelling, including an examination of the implications for future erosion rates if/where wind patterns and tide heights (sea level) are predicted to change. Sea level rise of 20 cm or greater could have a major impact on the patterns and rates of bank erosion, as well as the extent of inundation. It could also increase the erosional threat to the sea wall. We recommend that further work include a literature review of the predicted changes in sea level along the Victorian coast and an analysis of historical trends in storm events.

We did not analyse the clay mineralogy or the degree of shrink-swell of the clays forming the banks. However, the correlation between seasonal evaporation and the erosion rates recorded, strongly suggests that evaporation and its impact on wetting-drying of the bank surface leading to cracking of the clays is a major control on erosion that warrants further investigation. In particular, it would be important to establish whether there are distinct seasonal patterns in the degree of cracking of the surface during each low tide, and whether these patterns are controlled by evaporation. This could be established through experimental laboratory work using sediment samples and simulation of the range of climate conditions experienced at the site. Further measurement of the erosion pins over an additional 12 months or longer could also be undertaken to provide field evidence to establish whether the patterns in erosion rates recorded between November 2012 and November 2013 are indeed representative of an on-going seasonal pattern.

4.3 Options and recommendations for reducing erosion at Lang Lang

One of the main outcomes from this study was to identify management options to reduce sediment inputs from bank erosion into Western Port. The results and observations from the monitoring site demonstrate that these options need to address the physical erosion processes on the banks and/or slow/reduce wave energy at the bank surface (noting that further work to examine wave energy in more detail and establish thresholds, if they exist, is a recommended precursor). In evaluating the options, consideration should also be given to a number of other factors, namely:

- the likelihood of erosion continuing indefinitely through feedbacks, or at increased rates especially under predictions of future climate change;
- the likelihood of erosion threatening important infrastructure such as the sea wall;
- the impact on amenity, habitat and other environmental considerations;

- the cost of erosion remediation versus the environmental benefits of reducing sediment inputs into the bay; and,
- the relative contribution of bank erosion versus other sources of sediment inputs into the bay with respect to the new information and revised estimates of sediment yields presented here (this will be undertaken in a follow-on sediment study currently being planned by Melbourne Water and the CSIRO).

The options for reducing erosion of the banks at Lang Lang are presented in Table 12 and are summarised as follows:

1. Do nothing (this option should always be considered first).
2. Undertake simple works that encourage self-battering of the banks through slowing erosion and trapping sediment.
3. Undertake large-scale bank revetment to protect the banks from further erosion.
4. Undertake passive erosion control measures, primarily re-establishment of vegetation such as mangroves and other salt-tolerant species to increase roughness, improve wave energy absorption and enhance bank strength.
5. Install temporary or soft engineering breakwater structures such as geotextile tubes or Reef Balls on the tidal flats to reduce wave energy and trap sediment.
6. Install permanent hard engineering breakwater structures such as rip rap breakwaters or sheet piling structures.

It was beyond the scope of this study to undertake a further detailed investigation of the options including design plans and estimates of materials and costs. Recommended further reading includes:

- *Best Management Practices for Foreshore Stabilisation* (Swan River Trust, <http://www.swanrivertrust.wa.gov.au>), which includes several reports describing costs and a decision-making framework.
- *Coastal Engineering Manual* (US Army Core of Engineers, <http://chl.erd.c.usace.army.mil/cem>).

We recommend that all options be considered, including a 'do nothing' option, as well as a combination of revegetation and engineered breakwaters. Previous work in trying to establish mangroves at the site has shown that mangrove seedling survival rates are very low without the installation of structures or physical barriers that reduce wave energy near or around the plant (Hurst, 2013). This, along with the historical evidence (of an absence of mangroves) implies that wave energy is too high along the Lang Lang coastline for near shore vegetation establishment. Indeed further wave energy modelling may show that the wave energy parameters are too high for the survival of mature plants, even

Table 12. Management options to reduce erosion of the banks at Lang Lang and reduce sediment inputs into Western Port.

EROSION REMEDIATION OPTION	PROS	CONS
Do nothing	<ul style="list-style-type: none"> • Nil disturbance to the site or to local ecosystems. 	<ul style="list-style-type: none"> • Nil reduction of sediment inputs into the bay. • For many of the crenulations, erosion has already extended to the sea wall threatening this important infrastructure.
Undertake simple works on the banks, e.g. timber groynes, to encourage self-battering, trap sediment and reduce bank slope	<ul style="list-style-type: none"> • If designed well, these structures work with natural processes to achieve self-battering which is a good long-term solution for reducing bank erosion. 	<ul style="list-style-type: none"> • Unknown effect on erosion rates: may reduce wave energy on the bank surface; conversely, may preferentially enhance turbulence and erosion around each structure. Will not trap large volumes of sediment since most are fines and easily resuspended.
Undertake large-scale revetment works on the banks e.g. rip-rap, concrete walls, gabion baskets, or sand-filled pillows	<ul style="list-style-type: none"> • Erosion rates would be significantly reduced (potentially to zero) depending on the materials used and design. 	<ul style="list-style-type: none"> • To date, revetment works using building waste have been undertaken by the landholders in some of the crenulations to protect the sea wall. It is clear that much of the material is inadequate (size and density) and on-going maintenance is required to patch areas that have continued to erode. • Large-scale bank revetment is likely to be very cost prohibitive, especially if natural rock of an appropriate size/density is used (instead of building waste). Hence, the effect on total sediment yields from erosion over the 8.6 km of coastline will be small.
Revegetation of the floodplain, banks or shoreline area using mangroves and/or other salt-tolerant species that are local to the area e.g. <i>Phragmites spp.</i> and <i>Melaleuca spp.</i>	<ul style="list-style-type: none"> • Revegetation has the potential to significantly reduce erosion through reduced wave energy, and/or through physically protecting the banks from erosion, and/or through providing root strength and enhanced resistance. • Revegetation provides additional environmental benefits (e.g. enhanced habitat) • 	<ul style="list-style-type: none"> • Mangrove planting at the site has been shown to have a very low success rate, although rates can be improved by using strong protective sleeves (e.g. polypipe) around plantings (Hurst, 2013). • Historical evidence shows that the shoreline was devoid of mangroves dating as far back as the 1800's and it is postulated that this is because wave energy is too great for mangrove establishment and survival at Lang Lang. • It is unknown whether wave energy would be less of a factor for other species such as <i>Phragmites</i> and <i>Melaleuca</i>, if they were planted on the upper banks and across the floodplain to the sea wall. High groundwater levels may instead be a key problem for their survival.
Installation of temporary or soft engineering structures off-shore to reduced wave energy (breakwaters) and trap sediment e.g. geotextile or coir tubes filled with sand, timber pile	<ul style="list-style-type: none"> • Off-shore breakwaters have the potential to significantly decrease wave energy and create calm(er), less erosive wave conditions in the near shore area, especially if they are installed as a continuous system over large areas. • Breakwaters also trap locally eroded sediment and sediment being 	<ul style="list-style-type: none"> • Many of the temporary or soft engineering structures (excepting reef balls) have a high likelihood of failure over time. On-going monitoring, maintenance and replacement would need to be factored into designs and costings. • The impacts on erosion and sediment yields will depend on the size

EROSION REMEDIATION OPTION	PROS	CONS
fields, mesh fencing, Reef Balls, floating pontoon structures	<p>transported through long-shore drift.</p> <ul style="list-style-type: none"> • Reef balls have a very low risk of failure and can be placed, removed and re-positioned relatively easily. They also provide habitat for fish and other marine organisms. 	<p>(length), continuity and longevity of the structure.</p>
Installation of permanent hard engineering structures off-shore to reduce wave energy (breakwaters) and trap sediment e.g. rip-rap or sheet piling structures	<ul style="list-style-type: none"> • Off-shore breakwaters have the potential to significantly decrease wave energy and create calm(er), less erosive wave conditions in the near shore area, especially if they are installed as a continuous system over large areas. • Breakwaters also perform the function of being good sediment traps. • 	<ul style="list-style-type: none"> • Large-scale installation of rip-rap and sheet piling breakwaters may be very cost prohibitive. The impacts of small structures on reducing erosion and sediment yields from the 8.6 km of coastline would be correspondingly very small assuming a modest budget.

if favourable conditions are created during establishment. The options need to be monitored and evaluated in terms of the likelihood of success, as well as by predicted short, medium and long-term outcomes.

In light of the lateral continuity of the sediments and the extensiveness of erosion over the 8.6 km at Lang Lang, small-scale or discontinuous structures may prove to be cost-prohibitive relative to the small benefits gained. However, consideration could be given to focusing structures (and revegetation) where: i) erosion is at or close to the sea wall or other assets, ii) erosion is fastest, such as around the headlands; and iii) where bank sinuosity is highest, i.e. the area exposed to erosion is large relative to the straight-line distance. By targeting these areas, this would maximise the reduction of sediment inputs to the bay relative to the size/length/cost of the structure. However, in any design, the spatial distribution of works should also be considered in the context of the overall net effect on erosion and sediment inputs. For example, there is a good argument in favour of targeting the larger crenulations since this would reduce the overall length of the banks exposed to erosion (recognising that the headlands will continue to erode). Whereas targeting works at the headlands in order to target the areas of fastest erosion, may actually serve to increase the overall erodible area by reinforcing and enhancing the crenulated pattern.

Further work should also consider the effects of erosion remediation options on seagrass survival and turbidity in the bay in the immediate and wider area, in the context of generally clockwise sediment movement in the northern bay. Water quality improvement may not automatically follow erosion remediation. Hydrodynamic modelling may assist water quality impact assessments. Any environmental impacts from actions to control erosion of the banks, need to be considered also. Such impacts may involve waterbirds, crustaceans and other marine life that are known to reside or visit the site.

The orientation of off-shore structures also needs further consideration given the strong seasonal wind-wave patterns. Typically structures would be placed parallel to the banks and at the monitoring site, this would directly intercept winds from the west that have the potential to produce the greatest wave power. This study has also shown that strong NW winds in winter and strong S-SW winds in summer are also very important drivers of erosion. Structures will need to factor in these wind directions relative to the coastline.

Consideration also needs to be given to the separate roles of water level and wave energy before installing structures. This type of cost-benefit analysis should establish by how much, removing wave energy with structures would reduce the erosion rate.

In terms of materials, natural materials (rock, timber) are always preferred over artificial for the reasons of aesthetics, environmental impacts/friendliness and habitat potential. However, an interesting option that could be investigated further is Reef Balls which are supplied by Reef Ball Australia (see <http://www.reefballaustralia.com.au/default.htm>). The balls are concrete based, but can achieve flexible configurations and may serve as habitat for some marine life. They also have a large number of size options which may be attractive given the likelihood of predicted sea level rise within the next years-decades, relative to the size of investment and lifespan expected of an erosion control structure.

4.4 Implications for other eroding areas around Western Port

Bank erosion at Lang Lang is known to be the largest contributor of sediment directly to Western Port compared to other eroding areas around the bay (not including tributary inputs). For this reason we have focused our data collection at this site, recognising that erosion from other areas, such as Balnarring, Somers, Jam Jerrup, Grantville and Coronet Bay, also contribute to the total sediment load in the bay.

The banks along the Lang Lang coastline feature a unique suite of sedimentary properties (e.g. sediment composition, cohesion/resistance, bulk density and shrink-swell) which exert a strong influence on erosion rates. The erosion rates calculated here however, cannot be assumed to be directly transferable to these other eroding areas, especially where the sedimentology is significantly different. For example, the erosion at Jam Jerrup is occurring at an area known at the Red Bluff which is composed of a very different sedimentology that includes a large proportion of sands and exposed bedrock and weathered material.

A major outcome from this study is that it has highlighted several controls on erosion that are directly relevant to these other sites. In addition to the sedimentology, these controls include wind direction,

evaporation, fetch and wave power relative to the general orientation of the banks. The areas of coastline with a long fetch, for the dominant NW, W and SW wind directions show a good correlation with the locations of bank erosion identified around the bay. Hence, it is suggested that these controls are the most likely cause of erosion at these sites. Some preliminary analysis of the wave modelling results was undertaken in this study for the Grantville and Jam Jerrup sites. This was undertaken to estimate the maximum range of wave power that was likely to occur and to examine the temporal variability in wave power between sites that occurred over the duration of the monitoring period. Other sites could be evaluated in a similar manner.

To the address bank erosion more broadly across Western Port, the framework of options presented in Table 12 could also be considered. Notwithstanding this, it would be prudent to undertake smaller-scale studies of these sites to generally characterise the sedimentology and confirm the dominant erosion processes (compared to Lang Lang). More detailed modelling of wave power at small spatial scales should also be undertaken at all sites in order to design effective structures that factor in local conditions.

References

- Bird, E.C.F., 1971. Mangroves as Land-Builders. *Victorian Naturalist*, 88: 189-197.
- Bird, E.C.F., 1986. Mangroves and intertidal morphology in Westernport Bay, Victoria, Australia. *Marine Geology*, 69: 251-271.
- Bird, E.C.F. and Barson, M.M., 1975. Shoreline changes in Westernport Bay. *Proceedings of the Royal Society of Victoria*, 87(1): 15-28.
- Bird, J.F., 1980. Geomorphological implications of flood control measures, Lang Lang River, Victoria. *Australian Geographical Studies*, 18(2): 169-183.
- Bulthuis, D.A., 1983. Effects of in situ light reduction on density and growth of the seagrass *Heterozostera tasmanica* in Western Port, Victoria, Australia. *Journal of Experimental Marine Biology and Ecology*, 67: 91-103.
- Bulthuis, D.A., Brand, G.W. and Mobley, M.C., 1984. Suspended sediments and nutrients in water ebbing from seagrass-covered and denuded tidal mudflats in a southern Australian embayment. *Aquatic Botany*, 20: 257-266.
- Butcher, A.D., 1979. The Westernport Bay Environmental Study. *Marine Geology*, 30: 1-10.
- Crouch, R.J., 1987. The relationship of gully sidewall shape to sediment production. *Australian Journal of Soil Research*, 25: 531-539.
- Gell, R.A., 1974. Shore development in the Lang Lang Area, Unpublished BSc(hons) thesis, University of Melbourne, Melbourne.
- Harris, J.E., Hinwood, J.B., Marsden, M.A.H. and Sternberg, R.W., 1979. Water movements, sediment transport and deposition, Western Port, Victoria. *Marine Geology*, 30: 131-161.
- Harris, J.E. and Robinson, J.B., 1979. Circulation in Western Port, Victoria, as deduced from salinity and reactive-silica distributions. *Marine Geology*, 30: 101-116.
- Hinwood, J.B., 1979. Hydrodynamic and transport models of Western Port Victoria. *Marine Geology*, 30: 117-130.
- Hinwood, J.B. and Jones, J.C.E., 1979. Hydrodynamic data for Western Port, Victoria. *Marine Geology*, 30: 47-63.
- Hurst, T., 2013. Enhancing the ecological health of Western Port. Mangrove planting for coastal stabilisation 2010-2013. Final Report., Melbourne Water.
- Hurst, T.A., 2012. The Lang Lang Coast. A preliminary investigation of coastal erosion rates, Melbourne Water Corporation, Melbourne.
- Marsden, M.A.H. and Mallett, C.W., 1975. Quaternary evolution, morphology and sediment distribution, Westernport Bay, Victoria. *Proceedings of the Royal Society of Victoria*, 87: 197-137.
- Marsden, M.A.H., Mallett, C.W. and Donaldson, A.K., 1979. Geological and physical setting, sediments and environments, Western Port, Victoria. *Marine Geology*, 30: 11-46.
- Melbourne Water, 2011. Understanding the Western Port Environment. A summary of current knowledge and priorities for future research, Melbourne Water, East Melbourne.
- Rohweder, J., Rogala, J.T., Johnson, B.L., Anderson, D., Clark, S., Chamberlin, F., Potter, D. and Runyon, K., 2012. Application of Wind Fetch and Wave Models for Habitat Rehabilitation and Enhancement Projects - 2012 Update., Contract report prepared for U.S. Army Corps of Engineers' Upper Mississippi River Restoration-Environmental Management Program.

- Sargeant, I., 1977. A review of the extent and environmental effects of erosion in the Westernport Catchment, Environmental Studies Program, Publ. No. 174. Ministry for Conservation, Victoria.
- Shapiro, M.A., 1975. Westernport Bay Environmental Study 1973-1974, Ministry for Conservation Victoria, Melbourne.
- Shapiro, M.A. and Connell, D.W., 1975. The Westernport Bay Environmental Study. Proceedings of the Royal Society of Victoria, 87(1): 1-10.
- Smythe, G.D., 1842. Survey of the eastern coast of Western Port. Scale: 1:31679. Available at: Public Record Office Victoria, Victorian Archives Centre.
- Spencer-Jones, D., Marsden, M.A.H., Barton, C.M. and Carrillo-Rivera, J.J., 1975. Geology of the Westernport Sunkland. Proceedings of the Royal Society of Victoria, 87(1): 43-68.
- Sternberg, R.W. and Marsden, M.A.H., 1979. Dynamics, sediment transport and morphology in a tide-dominated embayment. Earth Surface Processes, 4: 117-139.
- Thompson, B.R., 1974. The geology and hydrogeology of the Western Port Sunklands, Geological Survey Report, number 1974/1, Mines Department Victoria.
- Victoria Department of Crown Lands and Survey, 1888. Yallock, County of Mornington. Scale 1:31,680. Available at: <http://nla.gov.au/nla.map-rm2741-439>
- Wallbrink, P.J., Hancock, G.J., Olley, J.M., Hughes, A., Prosser, I.P., Hunt, D., Rooney, G., Coleman, R. and Stevenson, J., 2003. The Western Port sediment study, Consultancy Report, CSIRO Land and Water, Canberra.

CONTACT US

t 1300 363 400
+61 3 9545 2176
e enquiries@csiro.au
w www.csiro.au

YOUR CSIRO

Australia is founding its future on science and innovation. Its national science agency, CSIRO, is a powerhouse of ideas, technologies and skills for building prosperity, growth, health and sustainability. It serves governments, industries, business and communities across the nation.

FOR FURTHER INFORMATION

CSIRO Land and Water
Dr Scott Wilkinson
t +61 2 6246 5582
e scott.wilkinson@csiro.au
w www.csiro.au/en/Organisation-Structure/Divisions/Land-and-Water.aspx